Supplementary Information (SI) for RSC Advances.
This journal is © The Royal Society of Chemistry 2025

Electronic Supplementary Information

Influence of the charge of 1,3,5-triaza-7-phosphaadamantane-based ligands on the anticancer activity of organopalladium complexes

Tommaso Lorenzon,[a] Maria Vescovo,[a] Michele Maiullari,[a] Giovanni Tonon,[b] Nuno Reis Conceição,[c] Sónia A. C. Carabineiro,[c,d] Abdallah G. Mahmoud,[d] Martin C. Dietl,[e] Nicola Demitri,[f] Laura Orian,[a] Pablo A. Nogara,[g] Isabella Caligiuri,[h] Flavio Rizzolio,[a,h] A. Stephen K. Hashmi,[e,i] Fabiano Visentin[b] and Thomas Scattolin*[a]

TABLE OF CONTENTS

NMR spectra.....2

X-ray diffraction analysis.....33

Computational details.....37

NMR SPECTRA

1D-NMR spectra were recorded on Bruker 300 Advance spectrometer. Chemical shifts values (ppm) are given relative to TMS (^{1}H and ^{13}C) and H_3PO_4 (^{31}P).

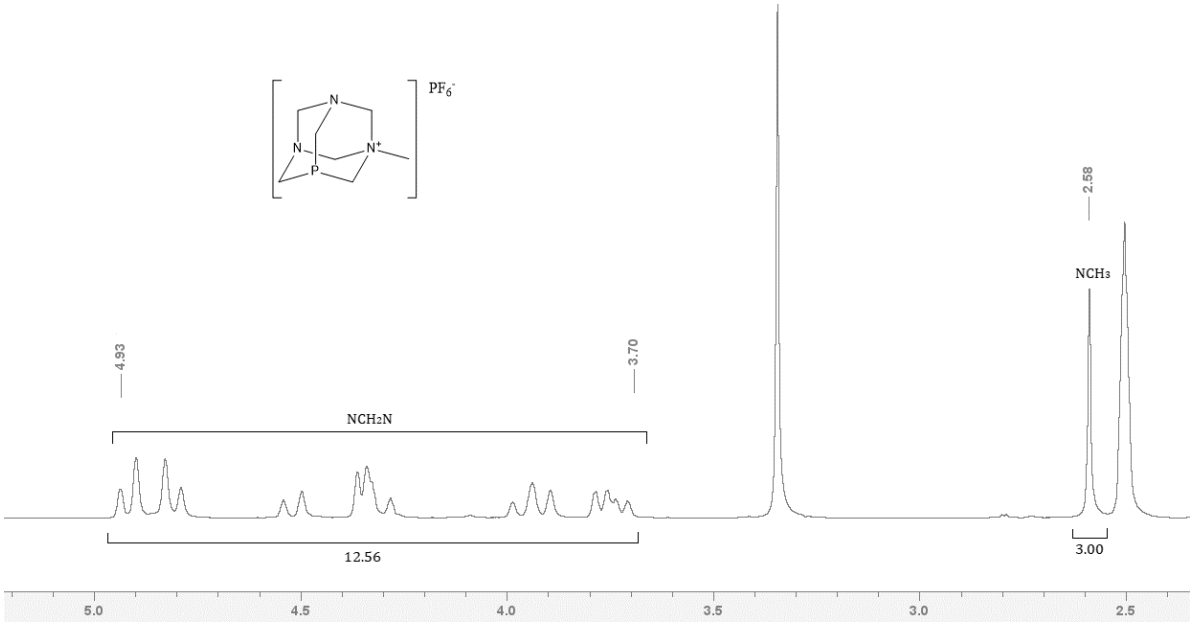

Figure S1. ^{1}H NMR spectrum of **b** in DMSO-d_6 at 298 K.

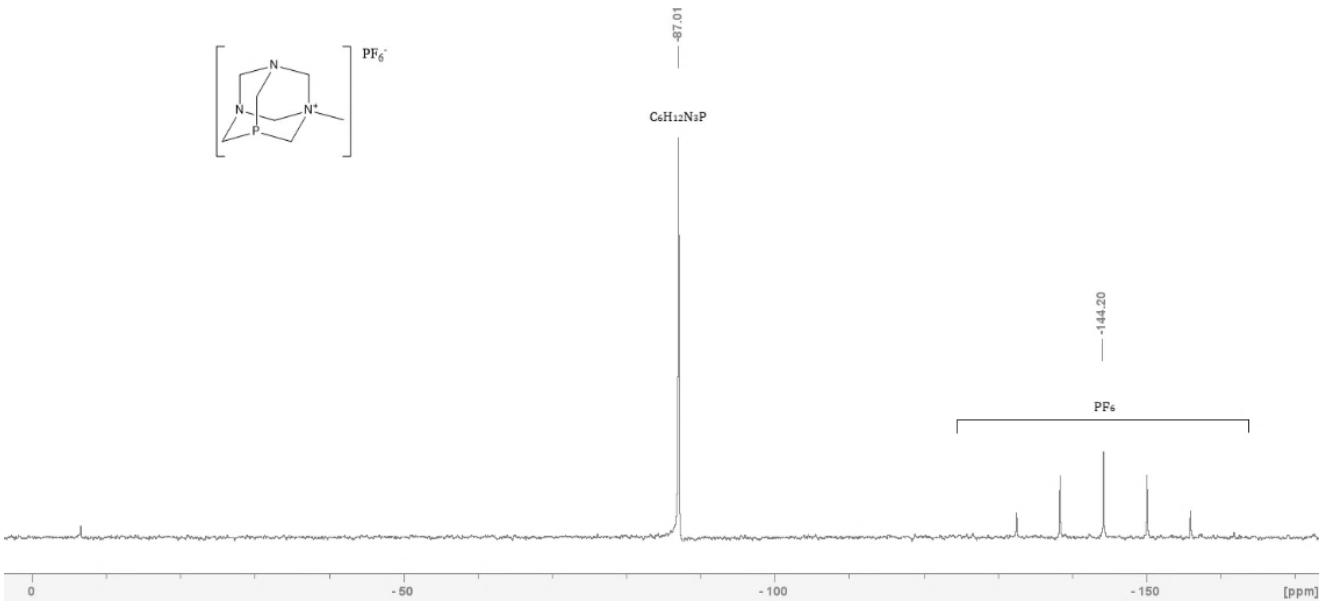

Figure S2. ^{31}P{^{1}H} NMR spectrum of **b** in DMSO-d_6 at 298 K

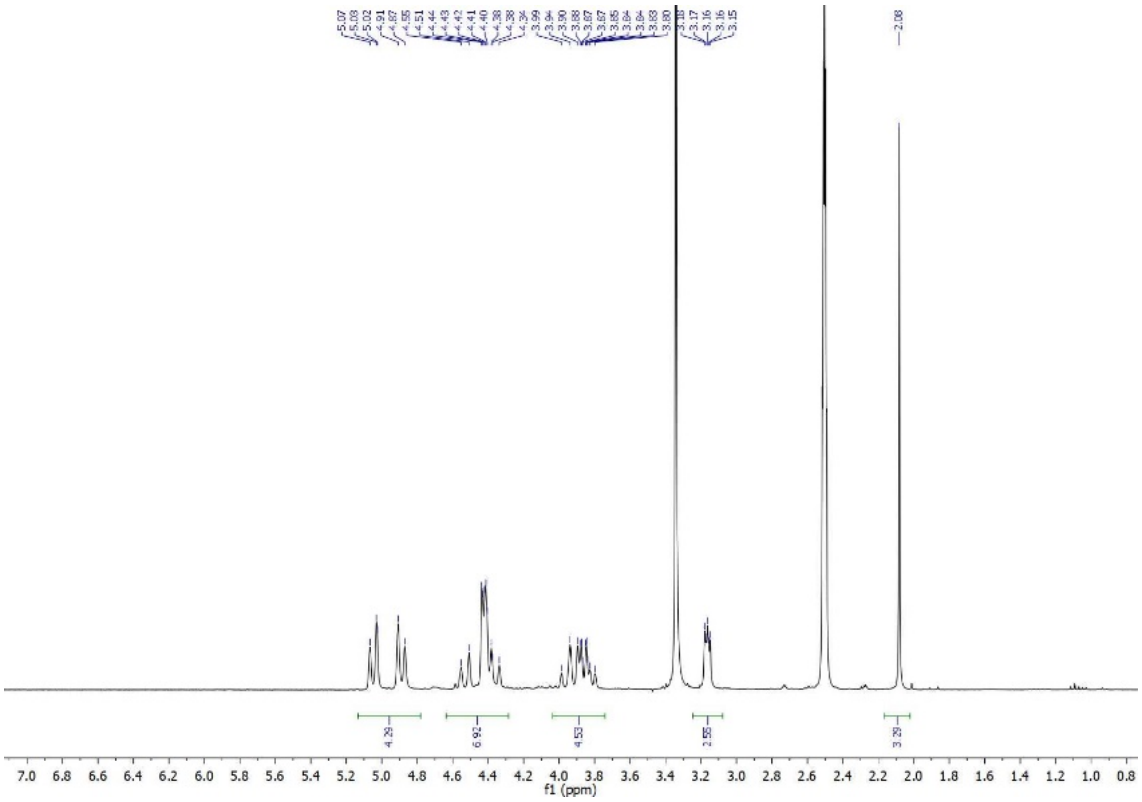

Figure S3. ^{1}H NMR spectrum of **c** in DMSO-d_6 at 298 K.

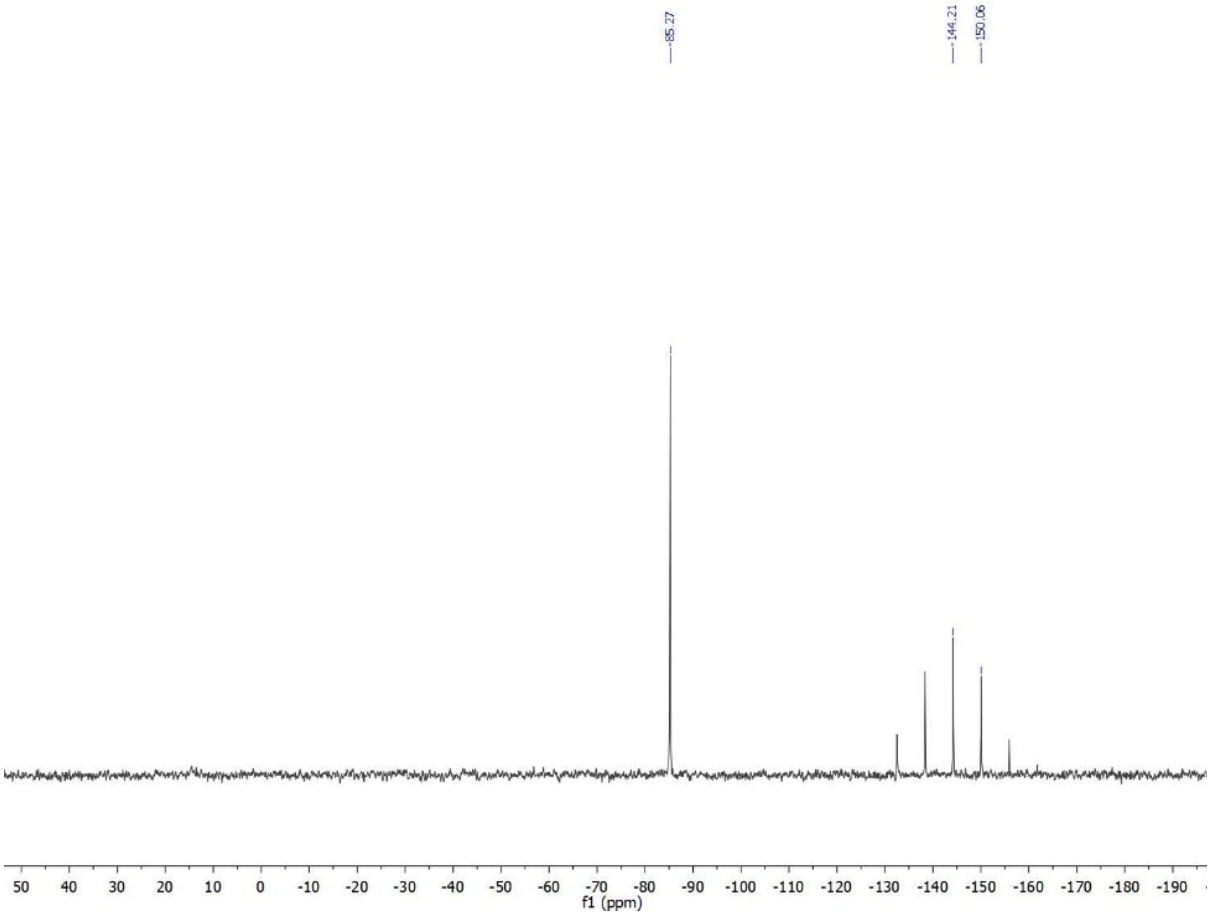

Figure S4. ^{31}P{^{1}H} NMR spectrum of **c** in DMSO-d_6 at 298 K

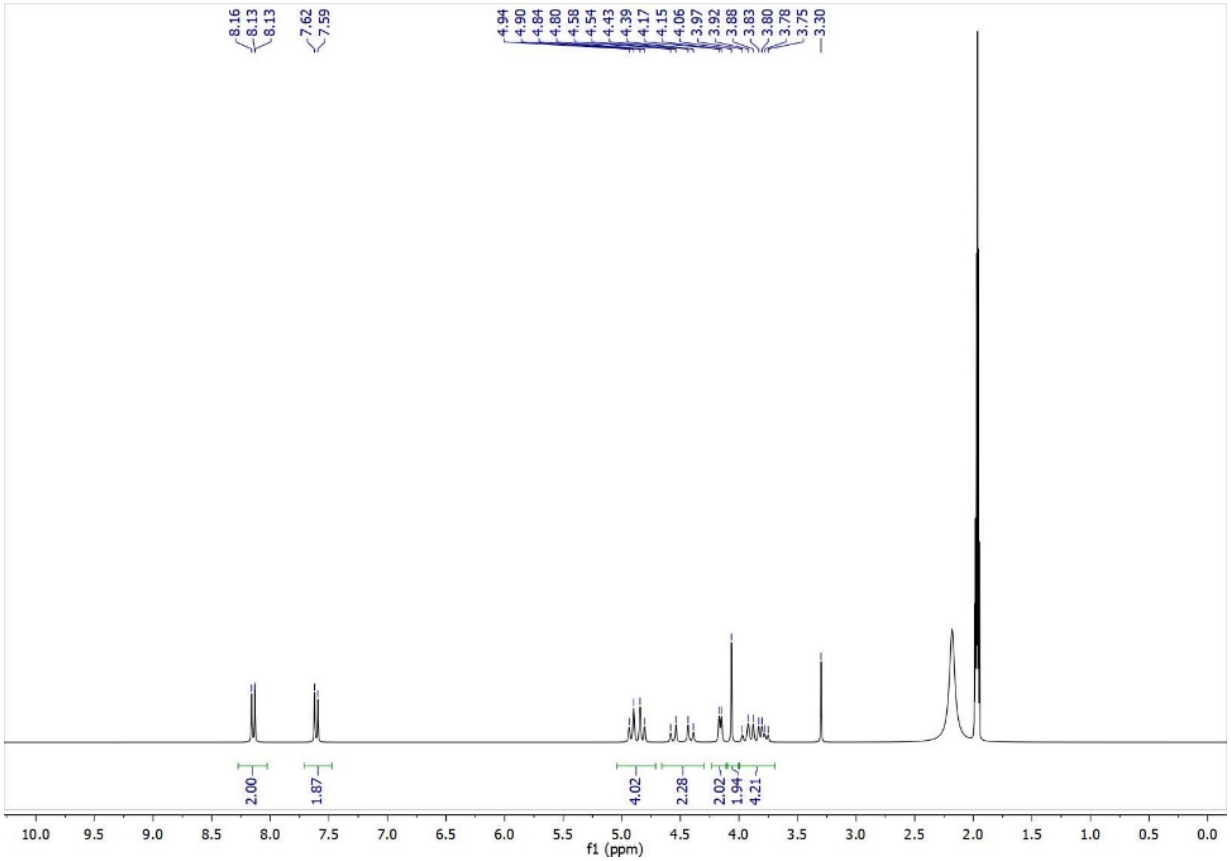

Figure S5. ^{1}H NMR spectrum of **d** in DMSO-d_6 at 298 K.

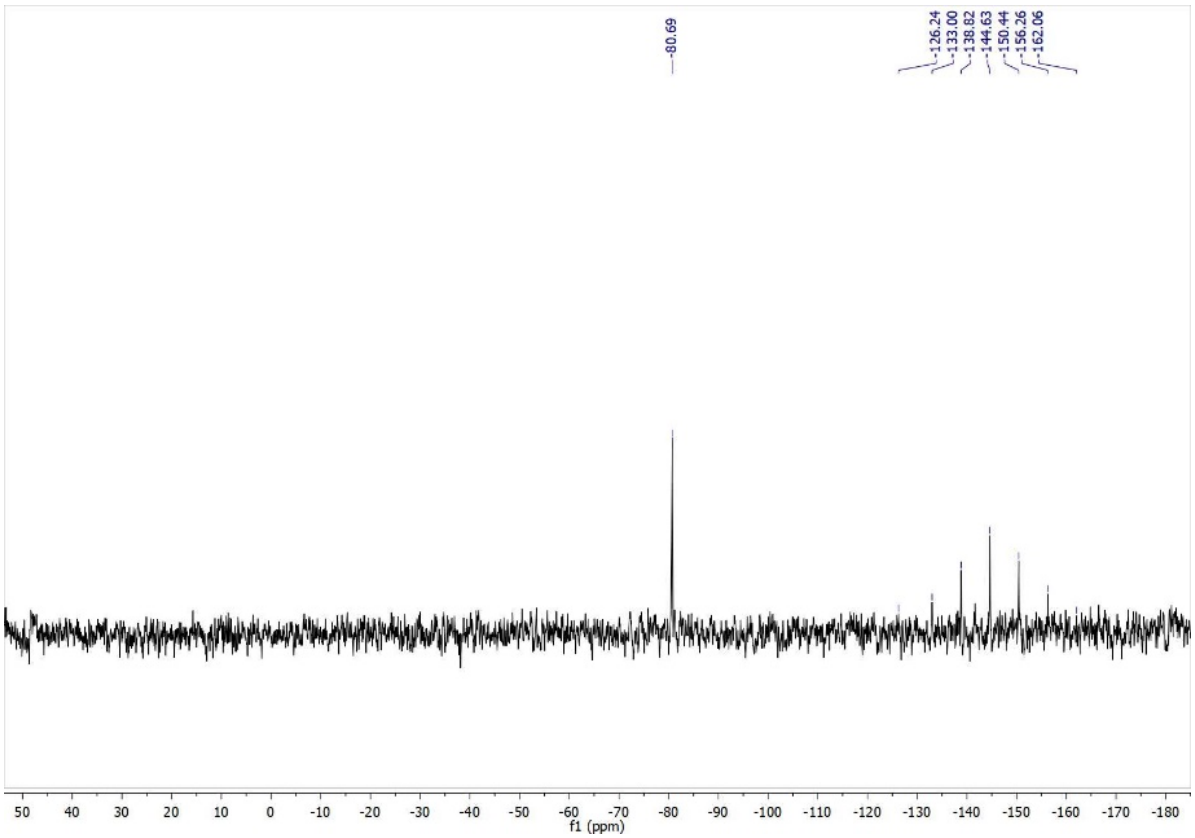

Figure S6. $^{31}P\{^{1}H\}$ NMR spectrum of **d** in DMSO-d_6 at 298 K

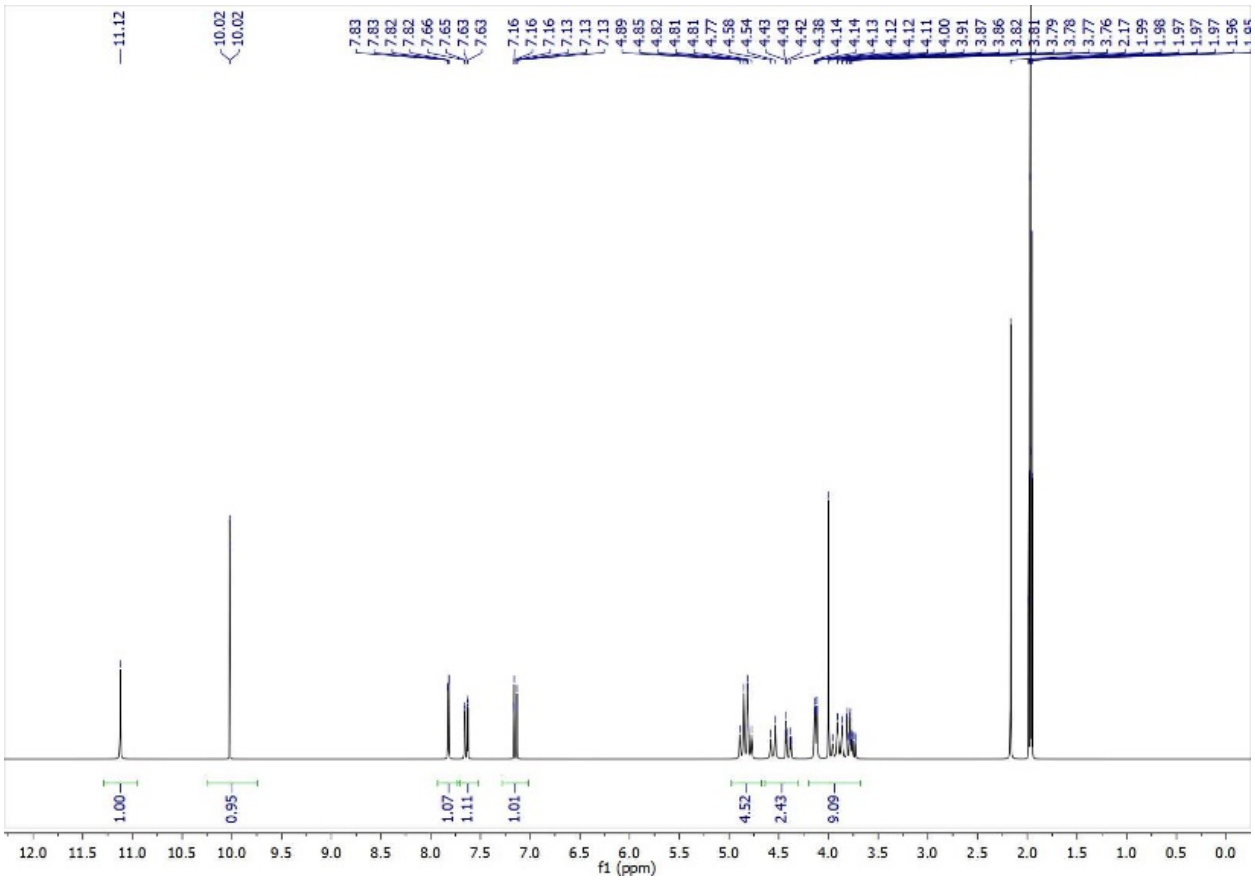

Figure S7. ^{1}H NMR spectrum of **e** in DMSO-d_6 at 298 K.

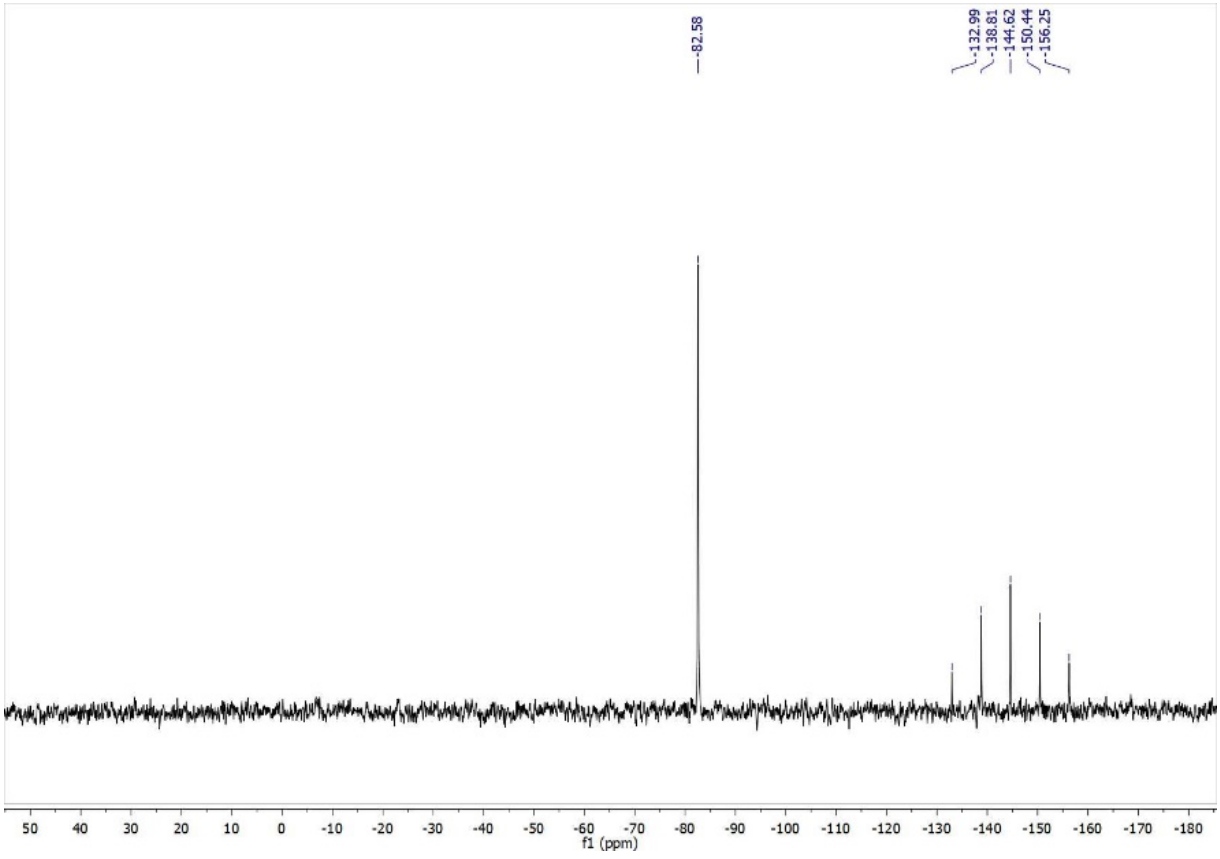

Figure S8. ^{31}P{^{1}H} NMR spectrum of **e** in DMSO-d_6 at 298 K

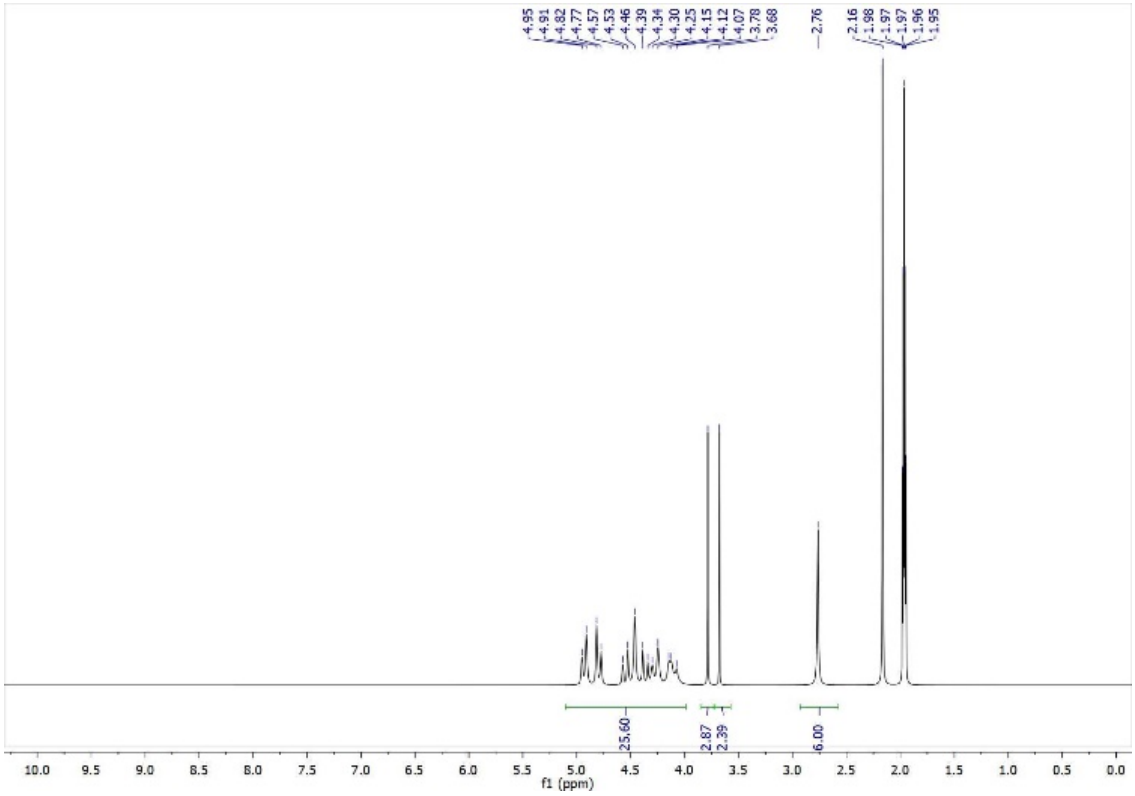

Figure S9. ^{1}H NMR spectrum of **3b** in CD_3CN at 298 K.

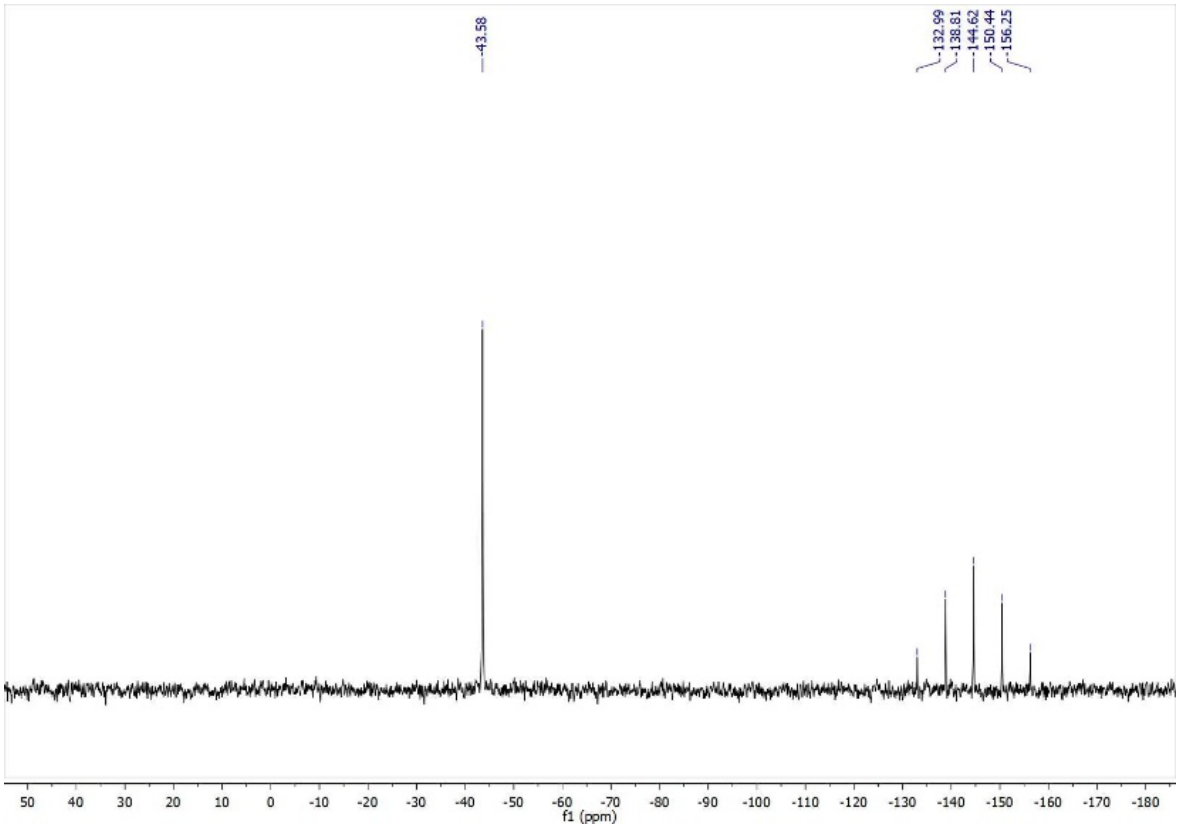

Figure S10. $^{31}P\{^{1}H\}$ NMR spectrum of **3b** in CD_3CN at 298 K

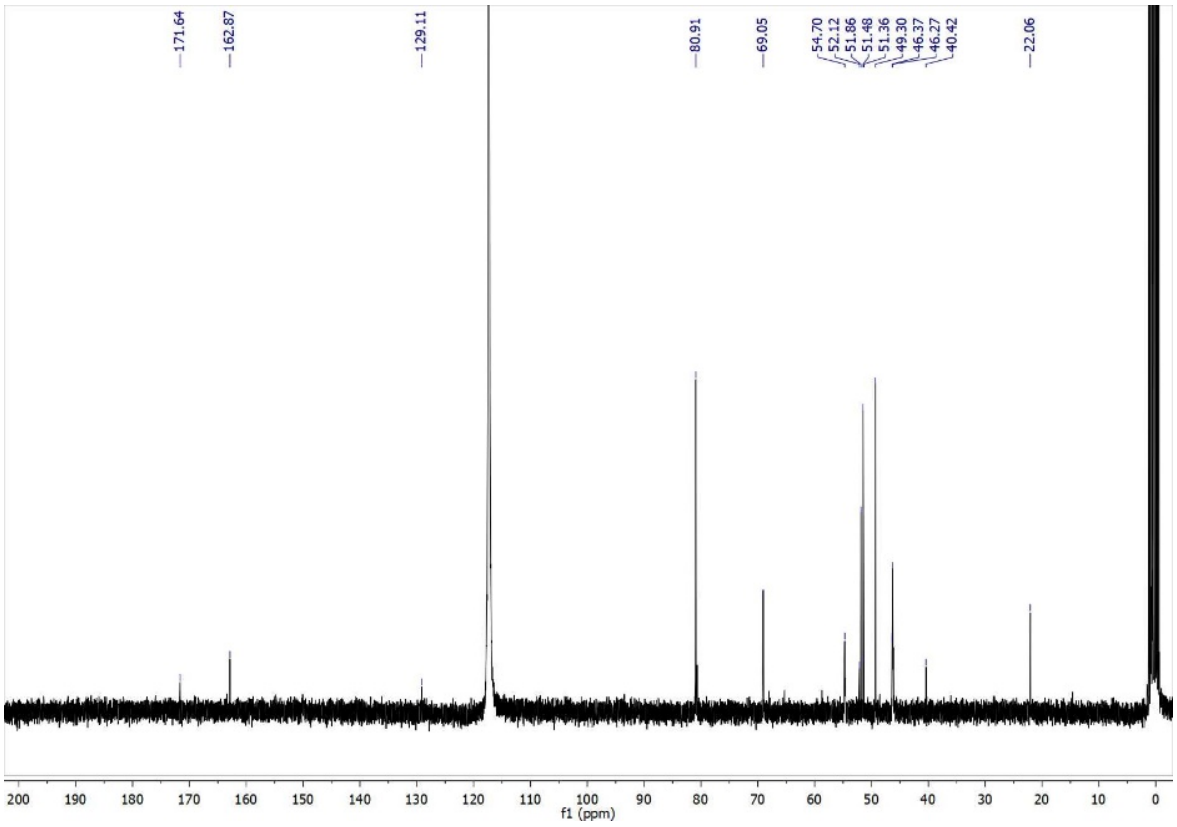

Figure S11. $^{13}C\{^{1}H\}$ NMR spectrum of **3b** in CD_3CN at 298 K

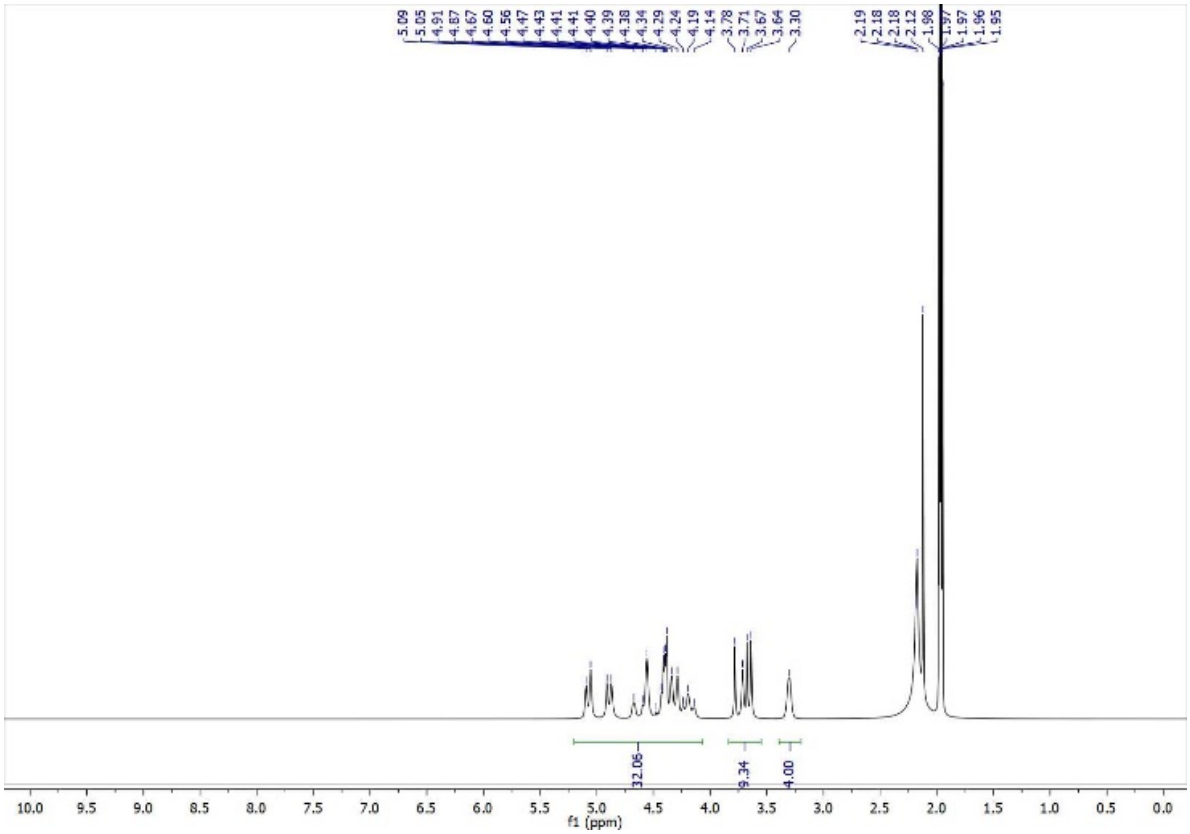

Figure S12. ^{1}H NMR spectrum of **3c** in CD_3CN at 298 K.

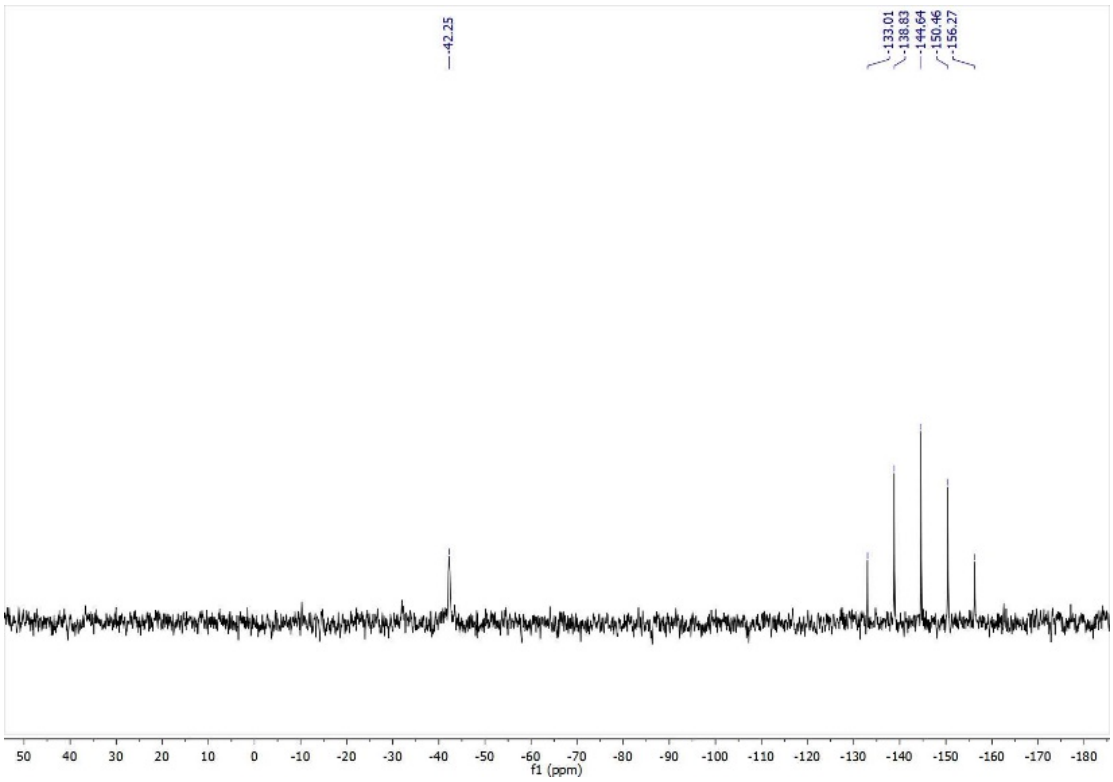

Figure S13. $^{31}P\{^{1}H\}$ NMR spectrum of **3c** in CD_3CN at 298 K

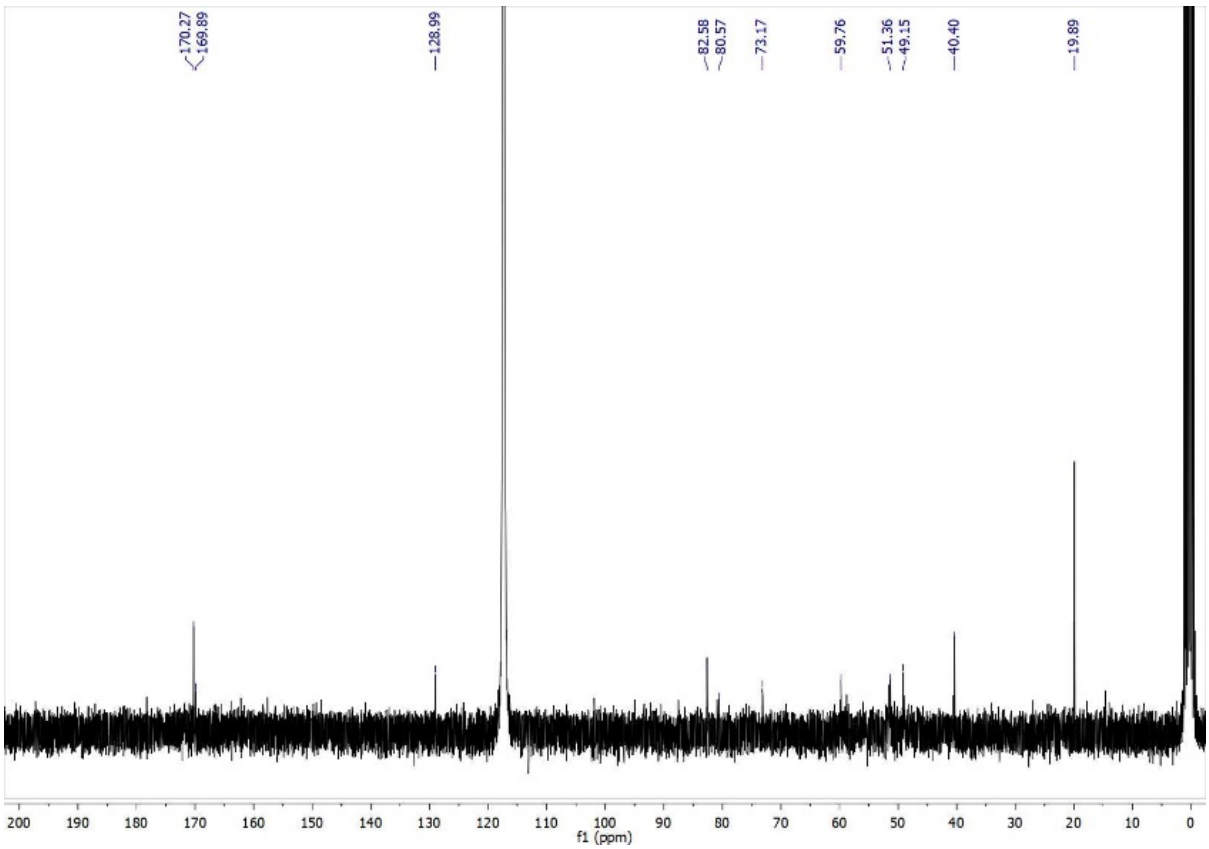

Figure S14. $^{13}C\{^{1}H\}$ NMR spectrum of **3c** in CD_3CN at 298 K

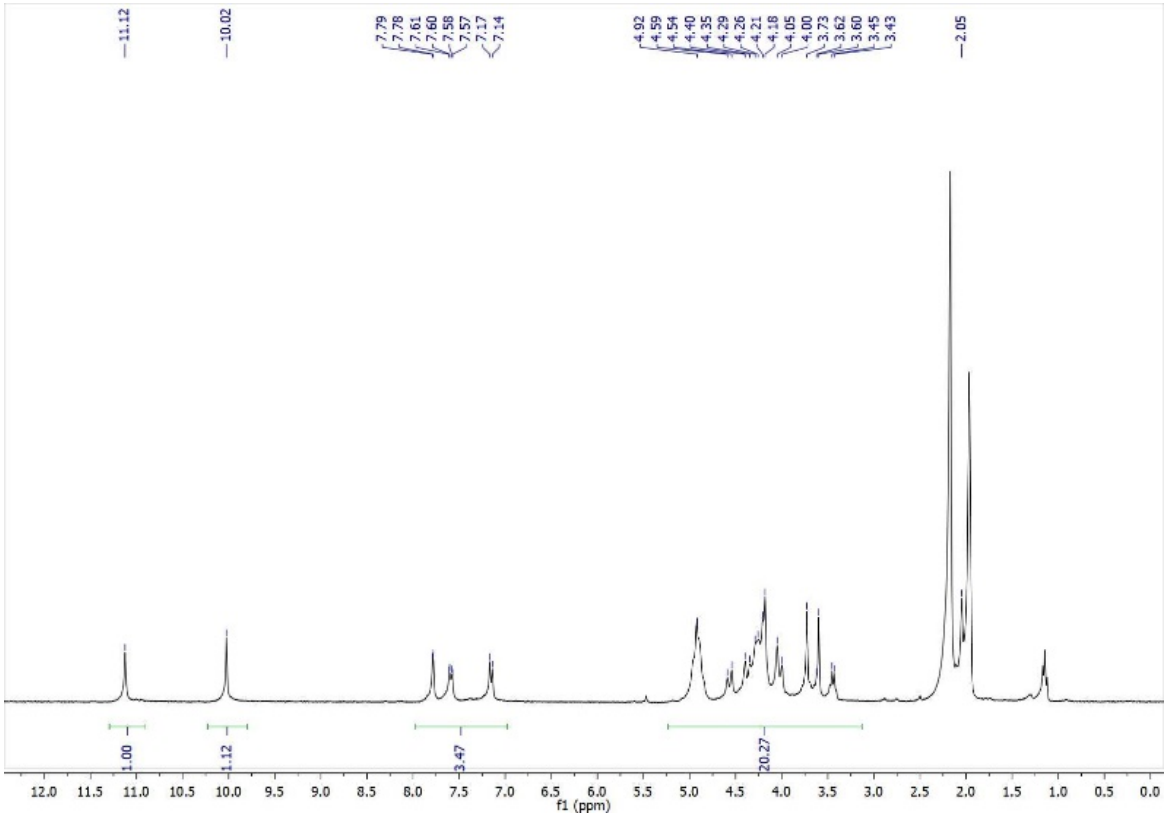

Figure S15. ^{1}H NMR spectrum of **3d** in CD_3CN at 298 K.

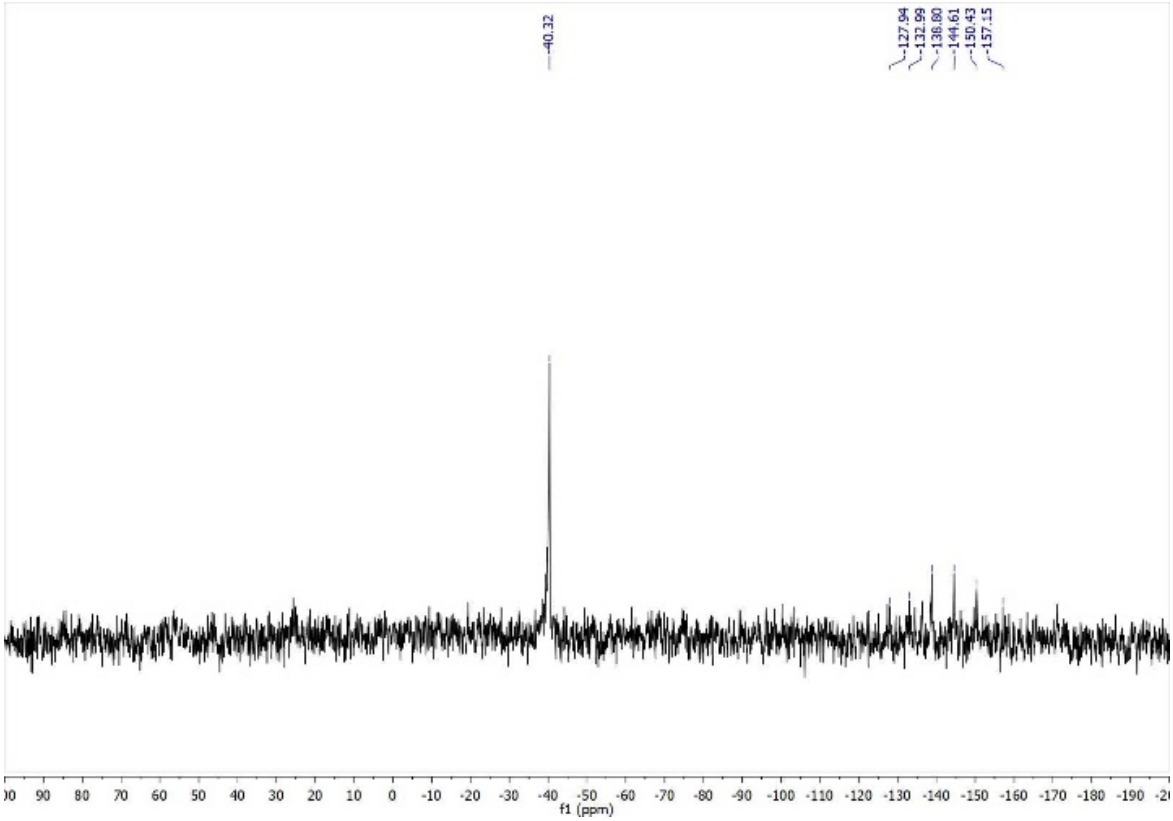

Figure S16. $^{31}P\{^{1}H\}$ NMR spectrum of **3d** in CD_3CN at 298 K

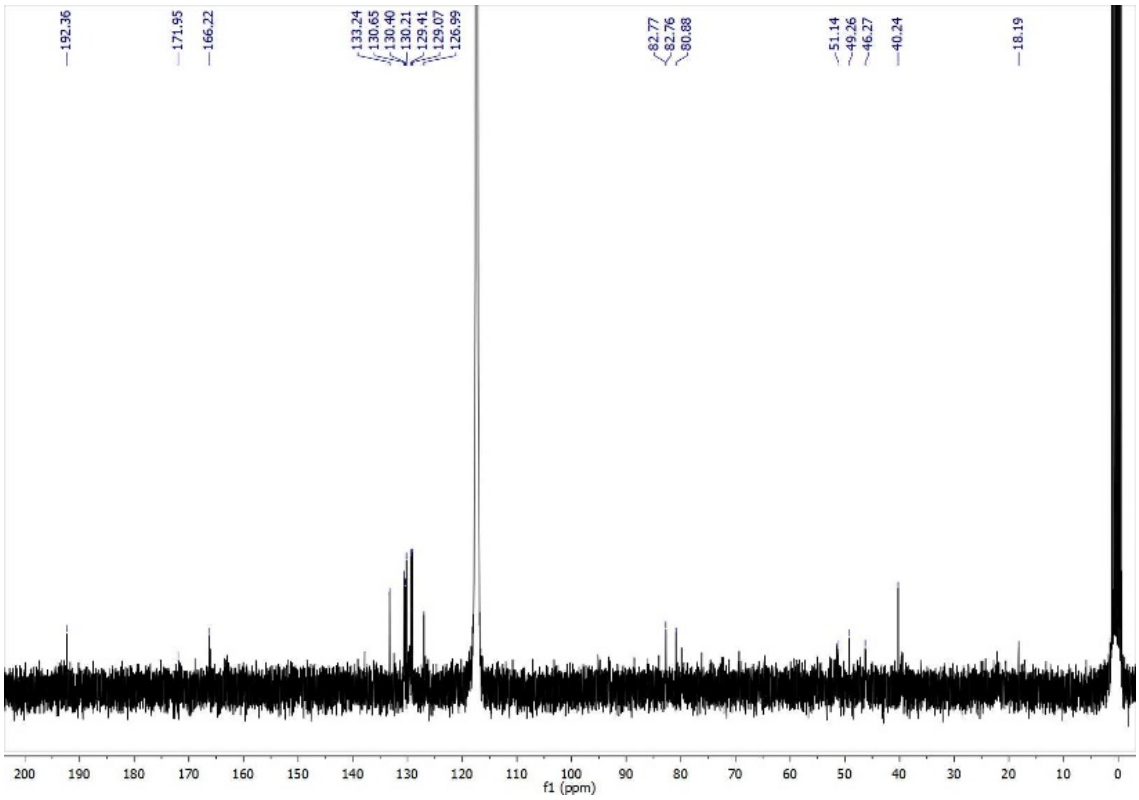

Figure S17. $^{13}C\{^{1}H\}$ NMR spectrum of **3d** in CD_3CN at 298 K

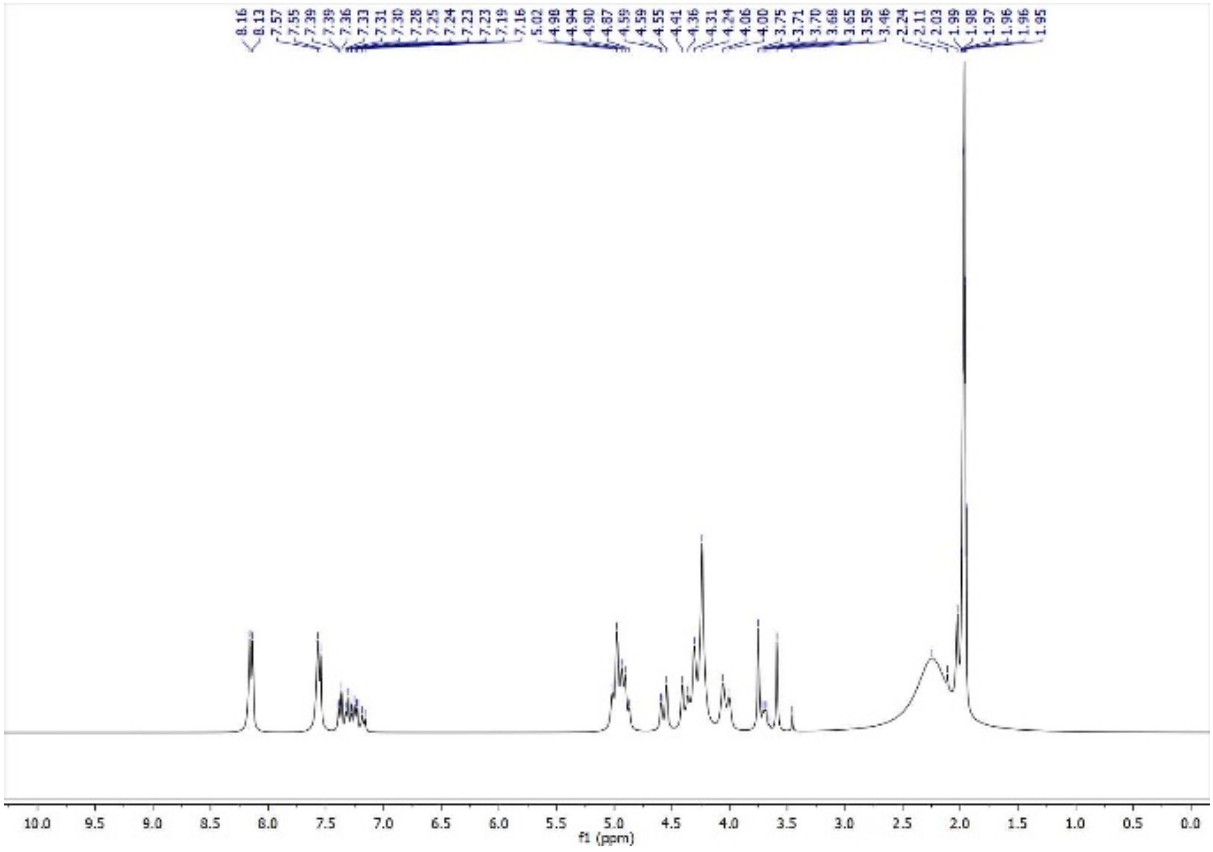

Figure S18. ^{1}H NMR spectrum of **3e** in CD_3CN at 298 K.

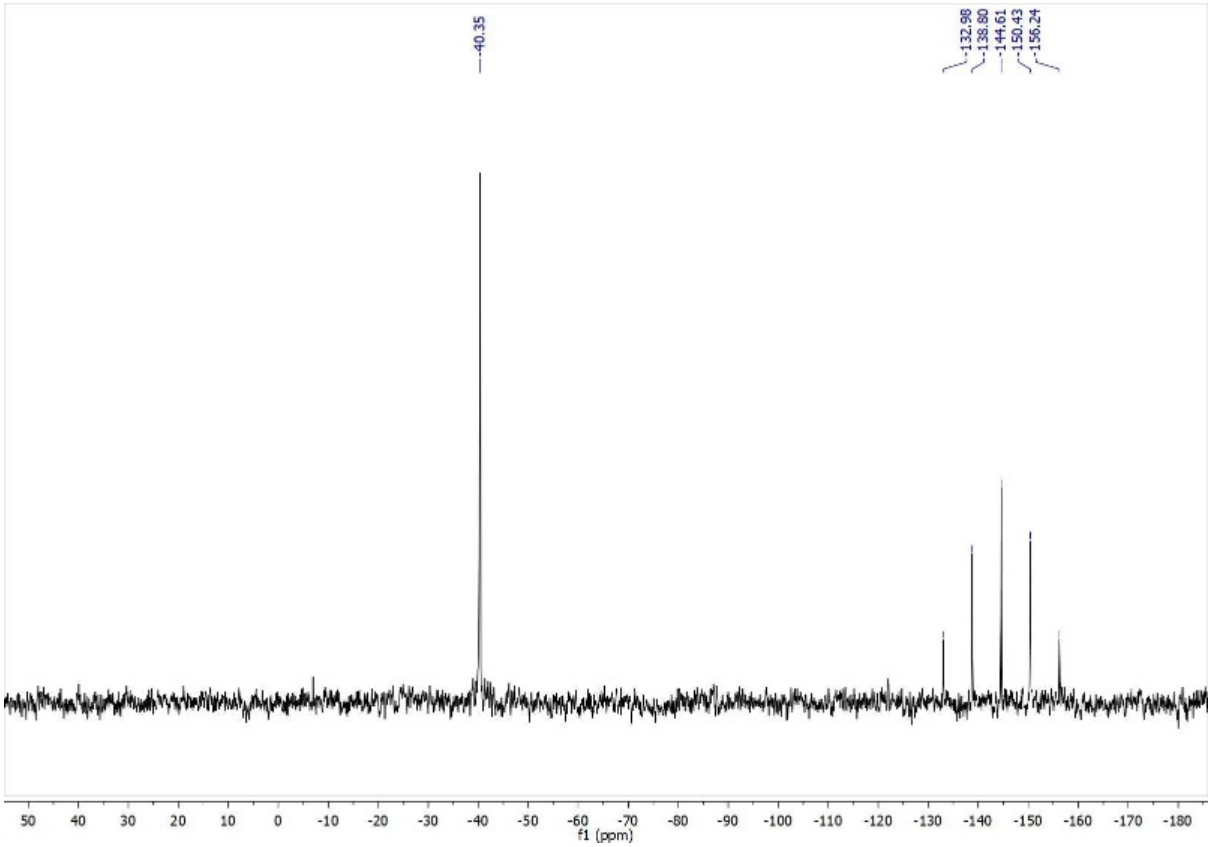

Figure S19. $^{31}P\{^{1}H\}$ NMR spectrum of **3e** in CD_3CN at 298 K

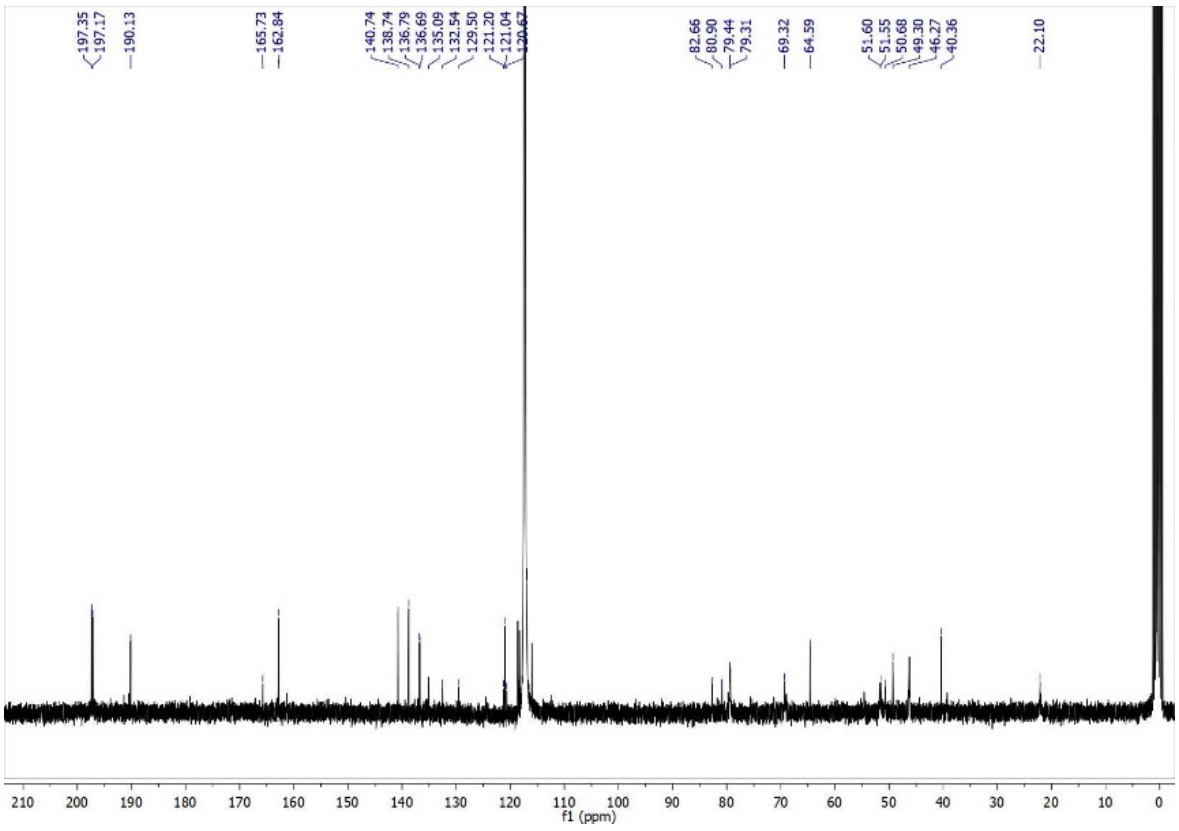

Figure S20. $^{13}C\{^{1}H\}$ NMR spectrum of **3e** in CD_3CN at 298 K

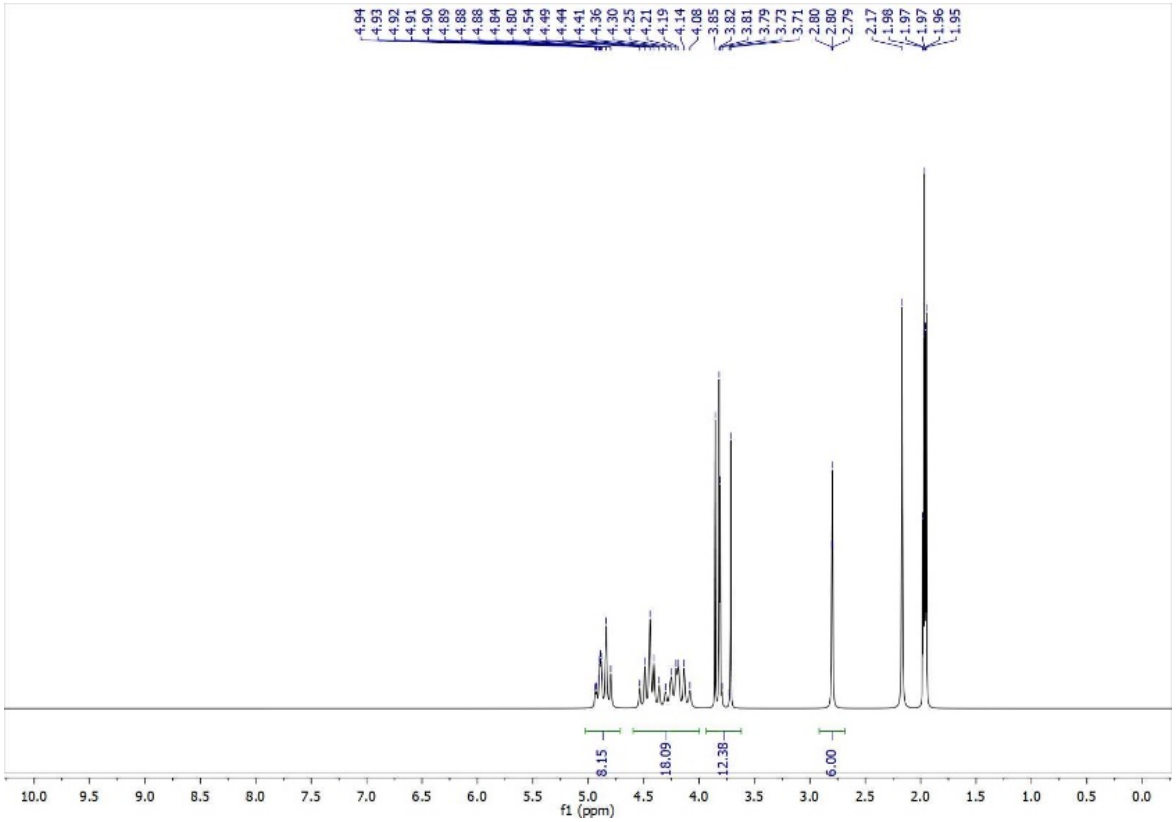

Figure S21. ^{1}H NMR spectrum of **4b** in CD_3CN at 298 K.

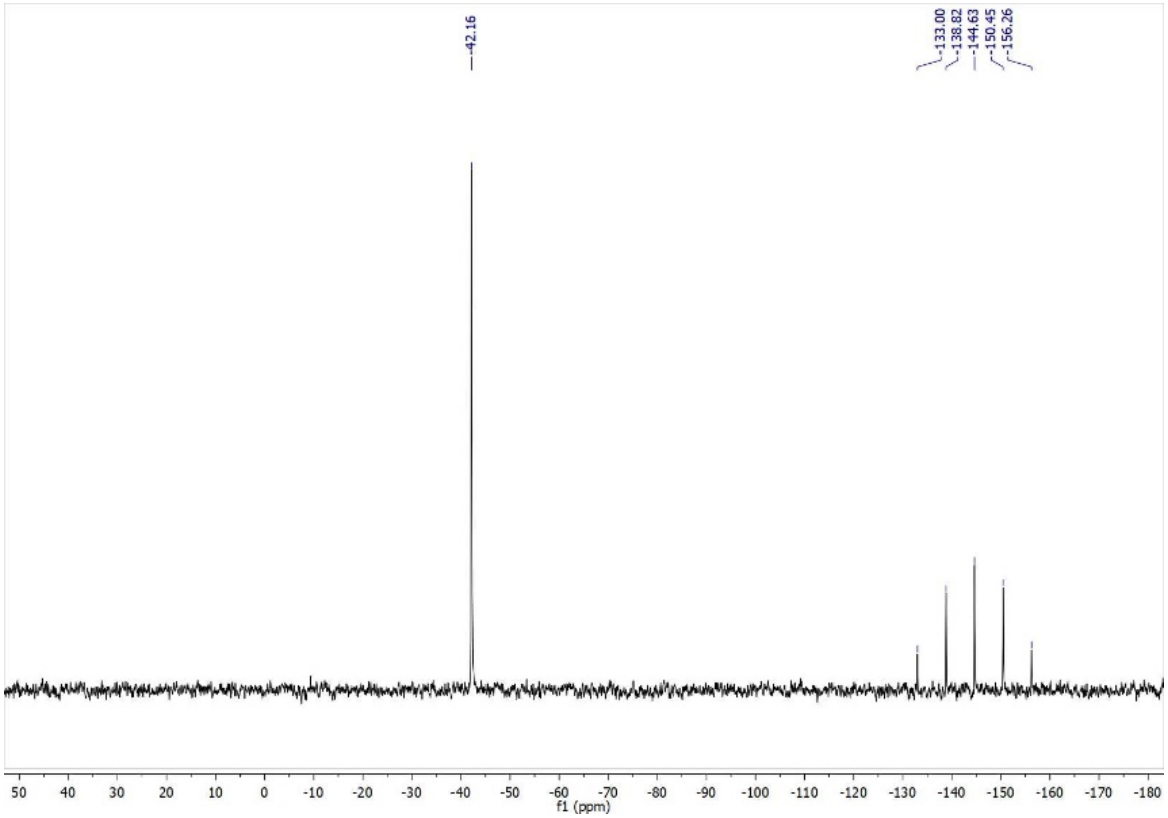

Figure S22. $^{31}P\{^{1}H\}$ NMR spectrum of **4b** in CD_3CN at 298 K

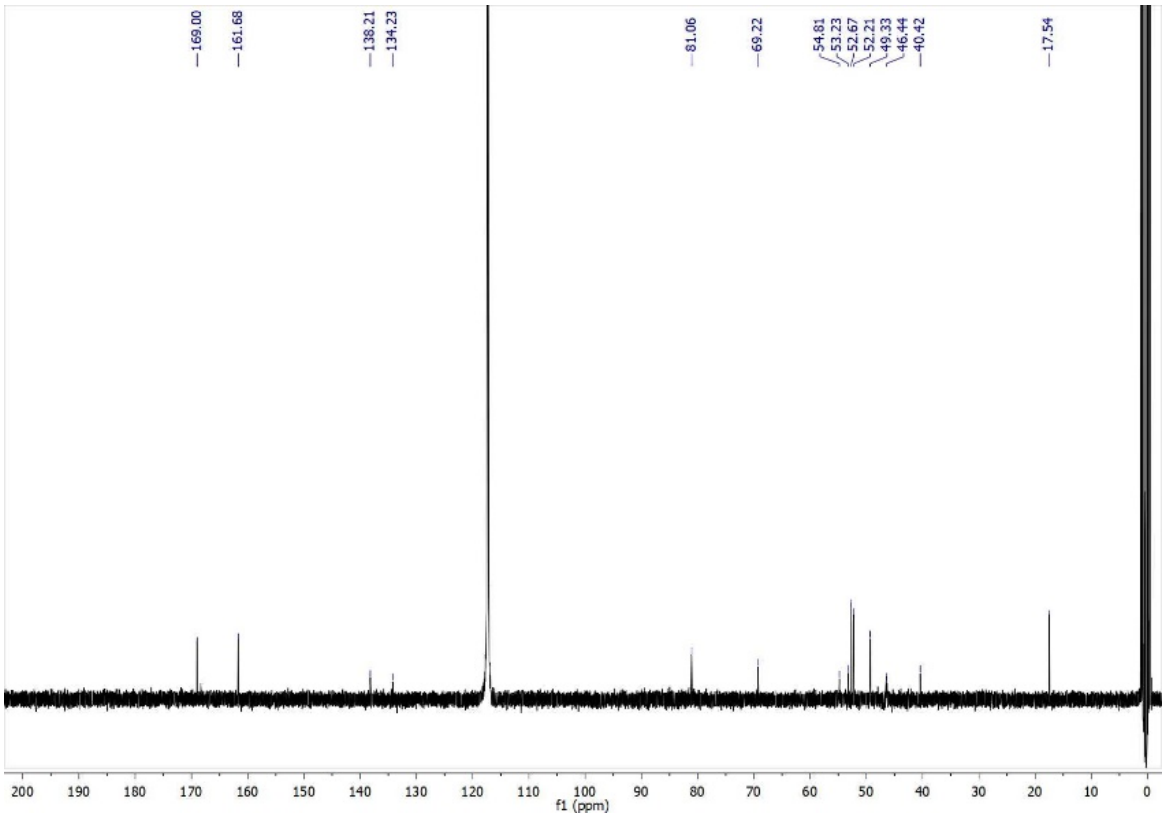

Figure S23. $^{13}C\{^{1}H\}$ NMR spectrum of **4b** in CD_3CN at 298 K

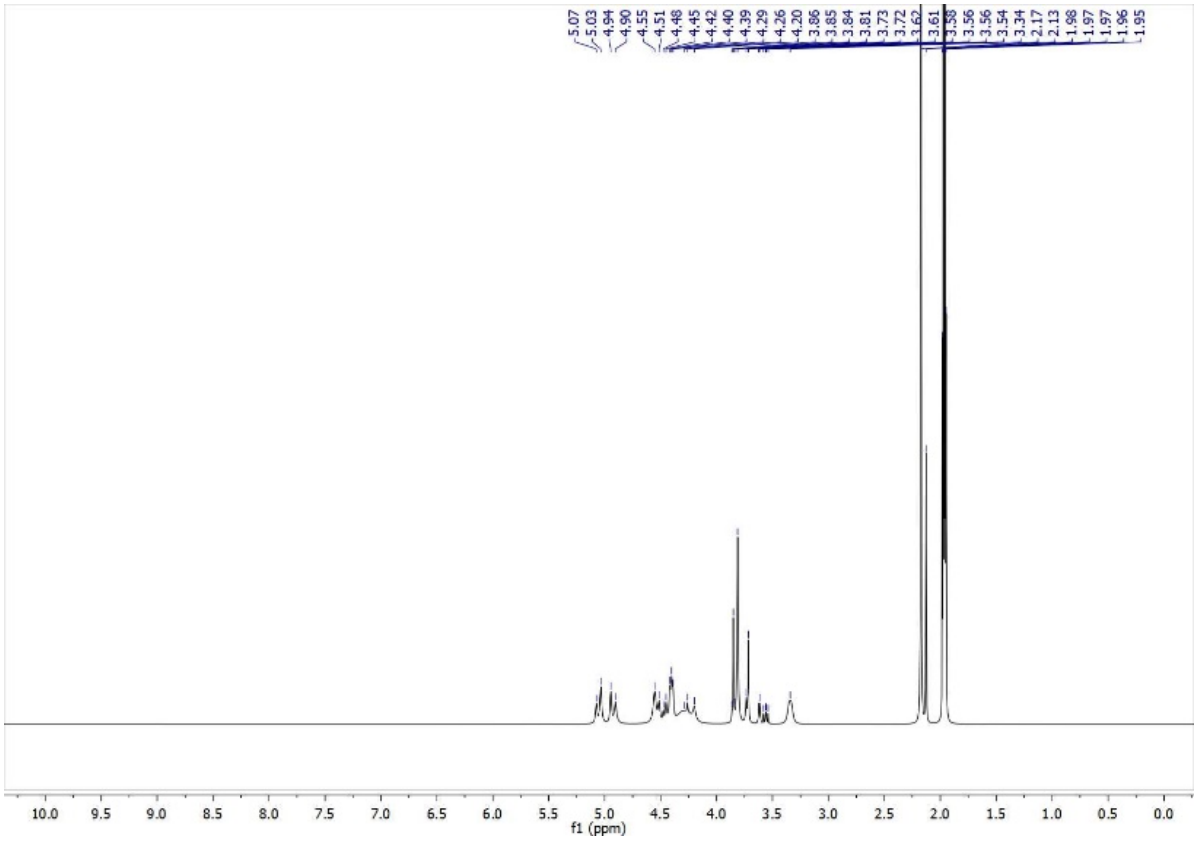

Figure S24. ^{1}H NMR spectrum of **4c** in CD_3CN at 298 K.

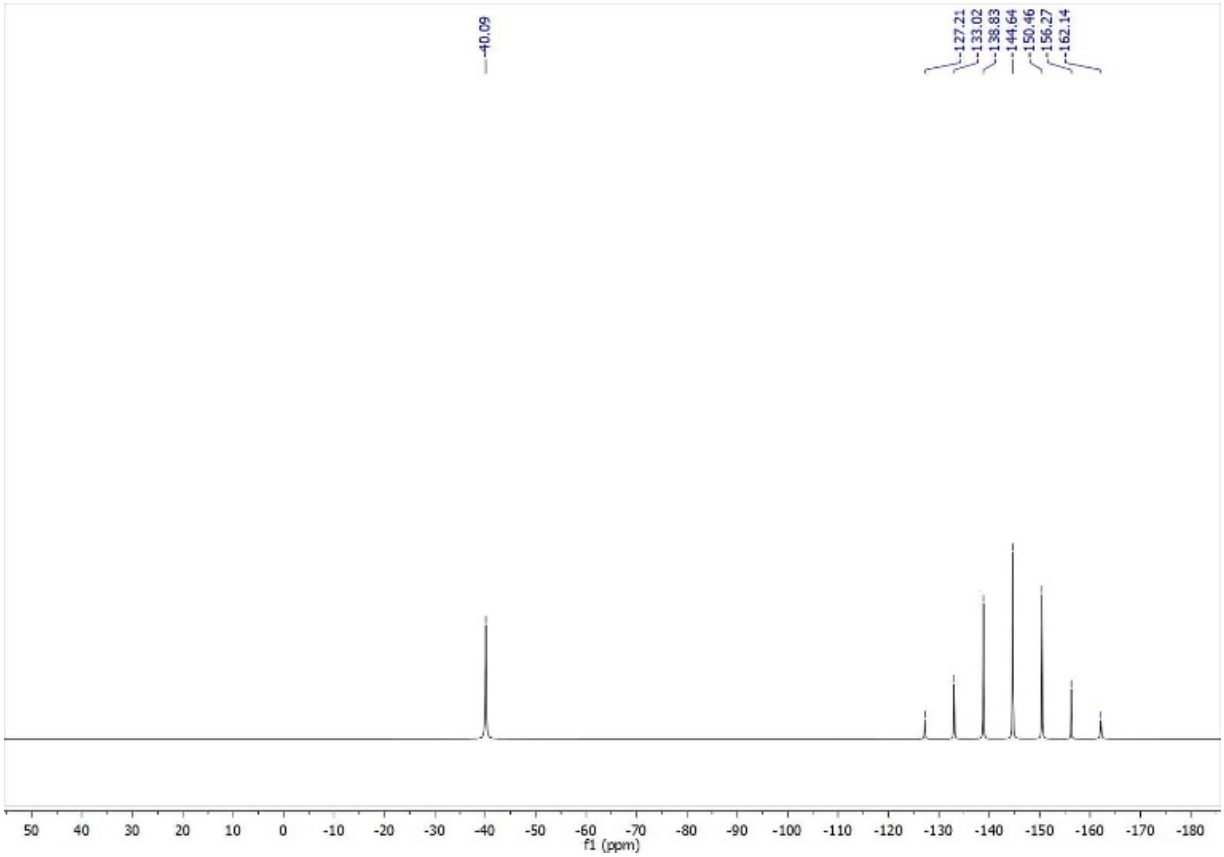

Figure S25. $^{31}P\{^{1}H\}$ NMR spectrum of **4c** in CD_3CN at 298 K

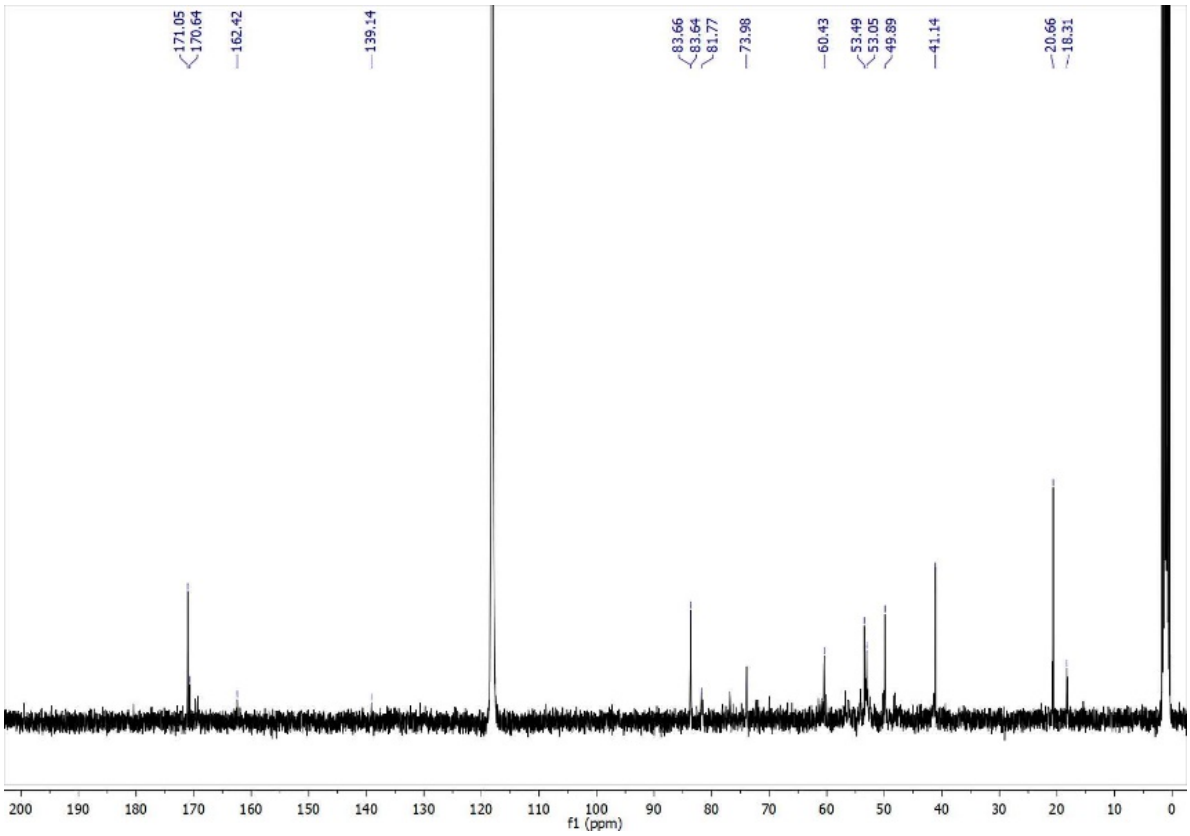

Figure S26. $^{13}C\{^{1}H\}$ NMR spectrum of **4c** in CD_3CN at 298 K

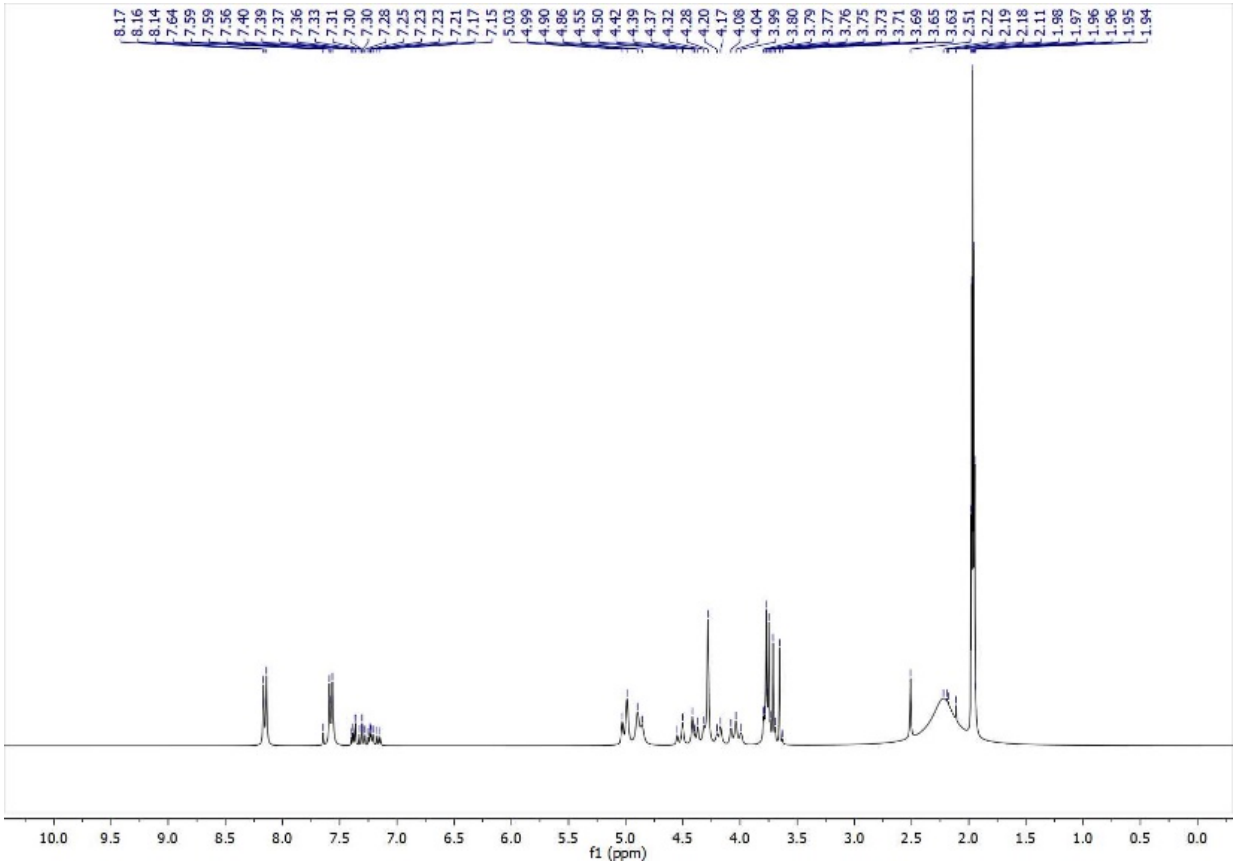

Figure S27. ^{1}H NMR spectrum of **4d** in CD_3CN at 298 K.

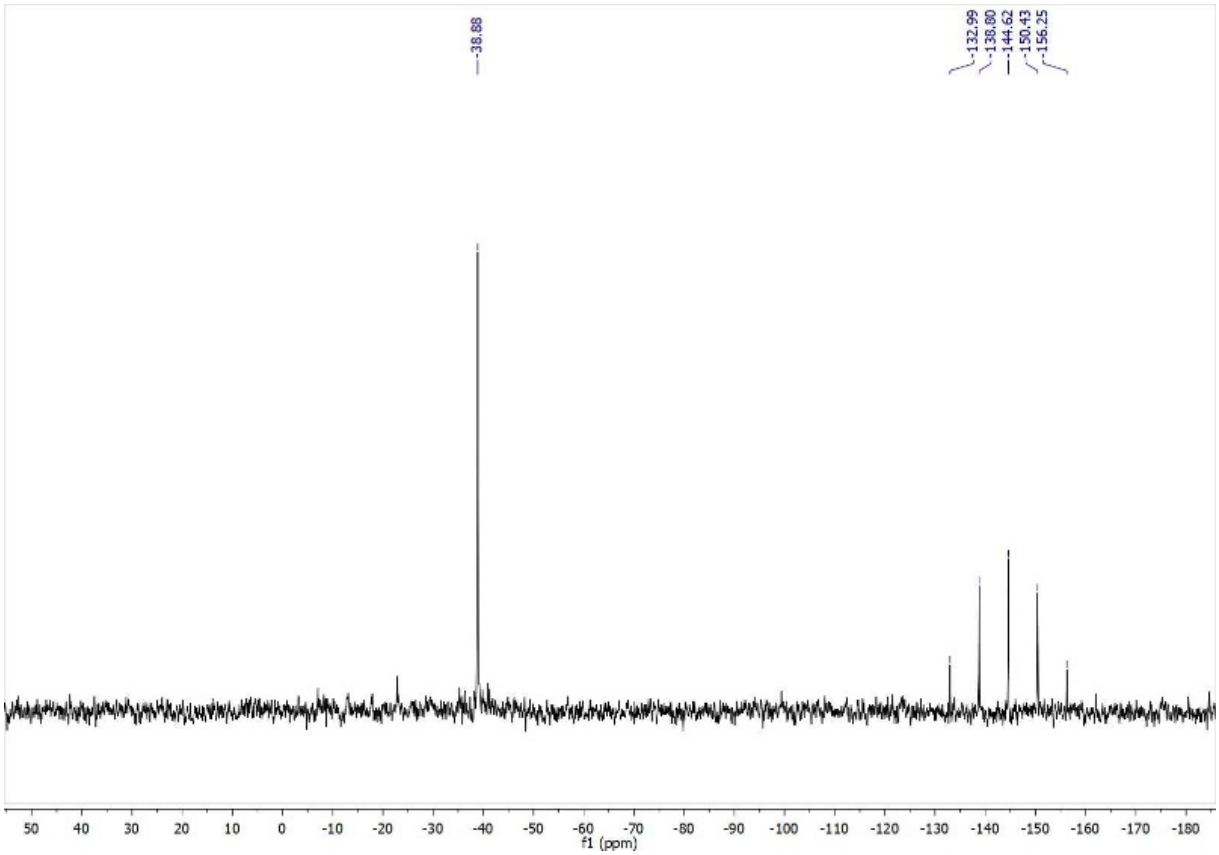

Figure S28. $^{31}P\{^{1}H\}$ NMR spectrum of **4d** in CD_3CN at 298 K

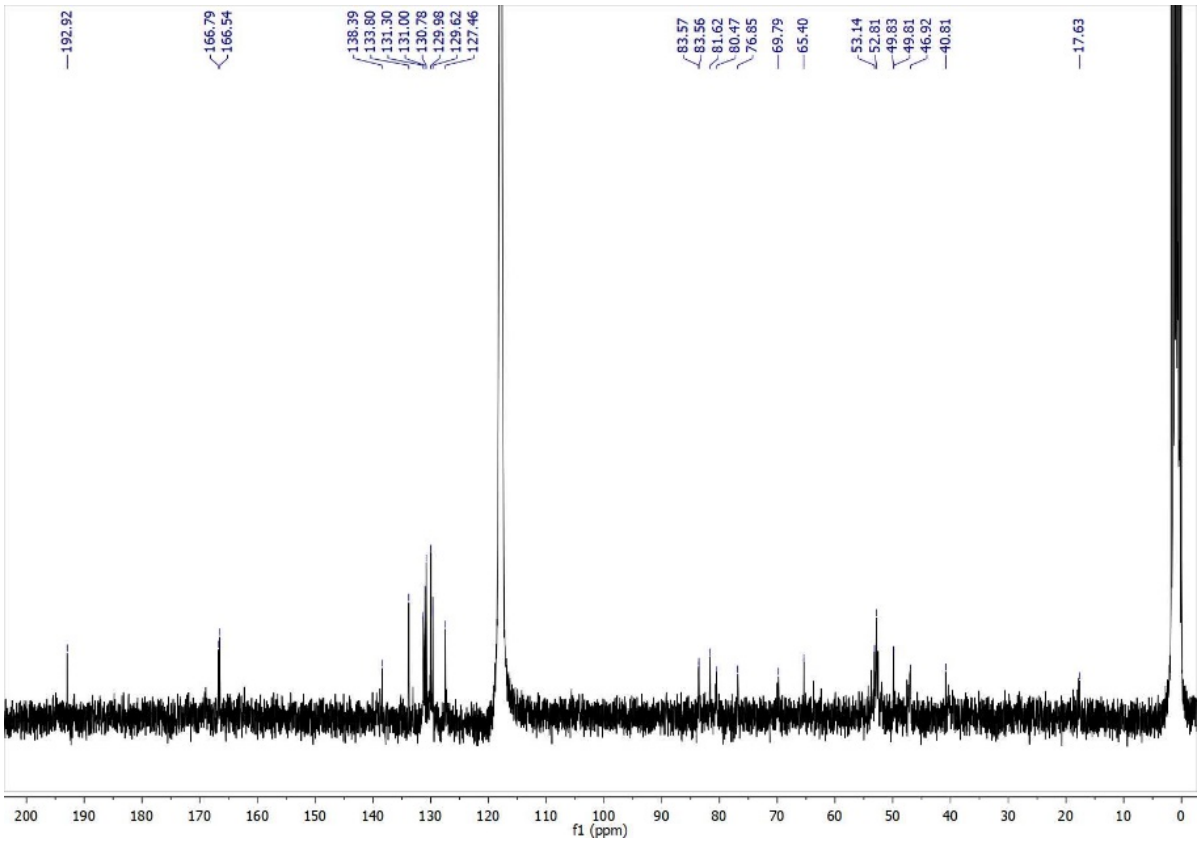

Figure S29. $^{13}C\{^{1}H\}$ NMR spectrum of **4d** in CD_3CN at 298 K

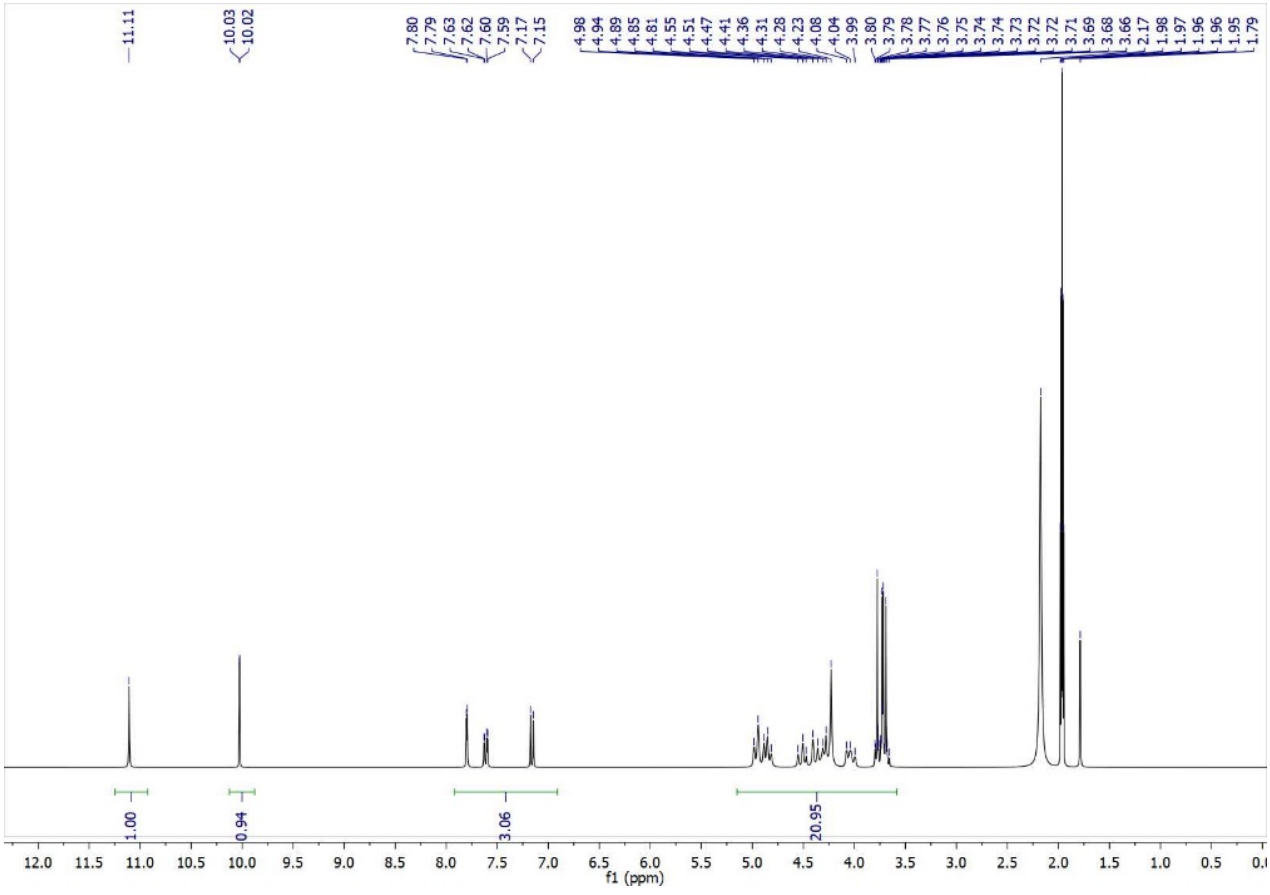

Figure S30. ^{1}H NMR spectrum of **4e** in CD_3CN at 298 K.

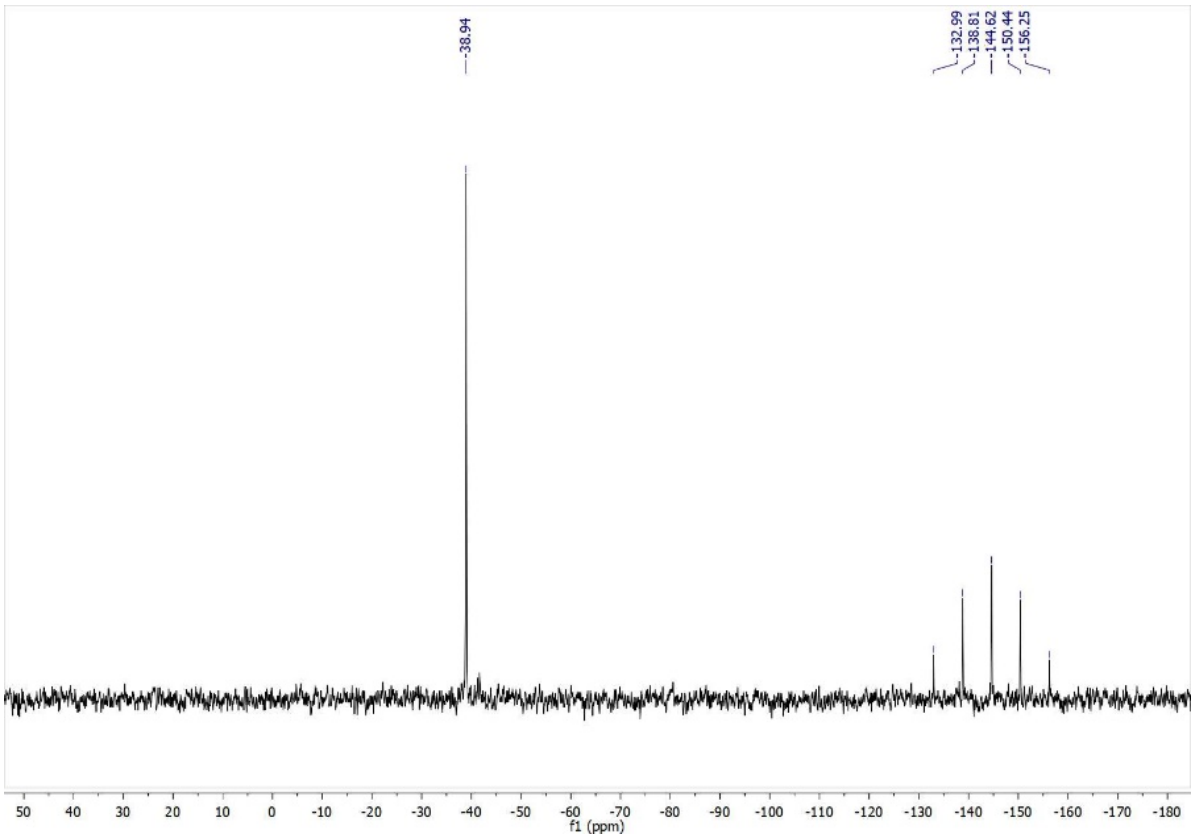

Figure S31. $^{31}P\{^{1}H\}$ NMR spectrum of **4e** in CD_3CN at 298 K

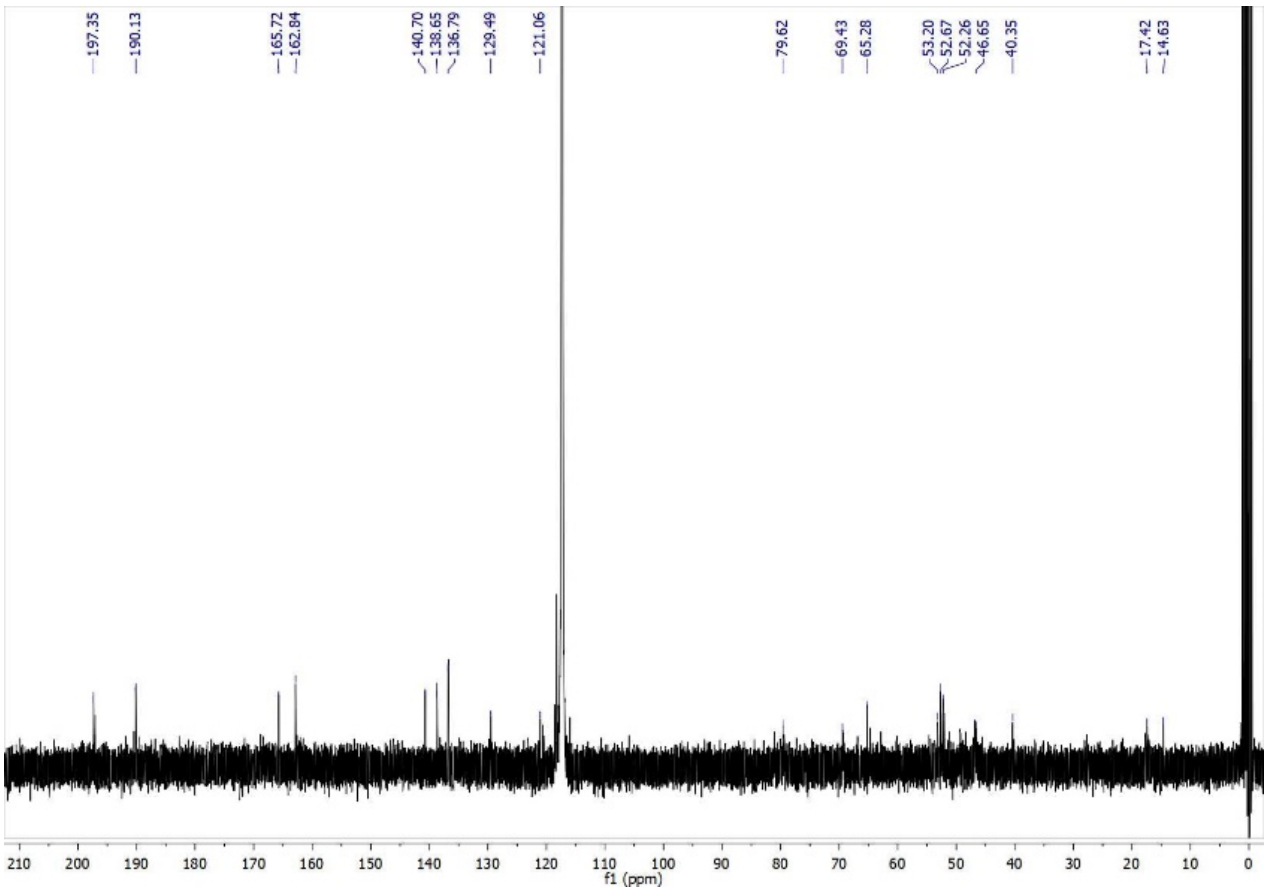

Figure S32. $^{13}C\{^{1}H\}$ NMR spectrum of **4e** in CD_3CN at 298 K

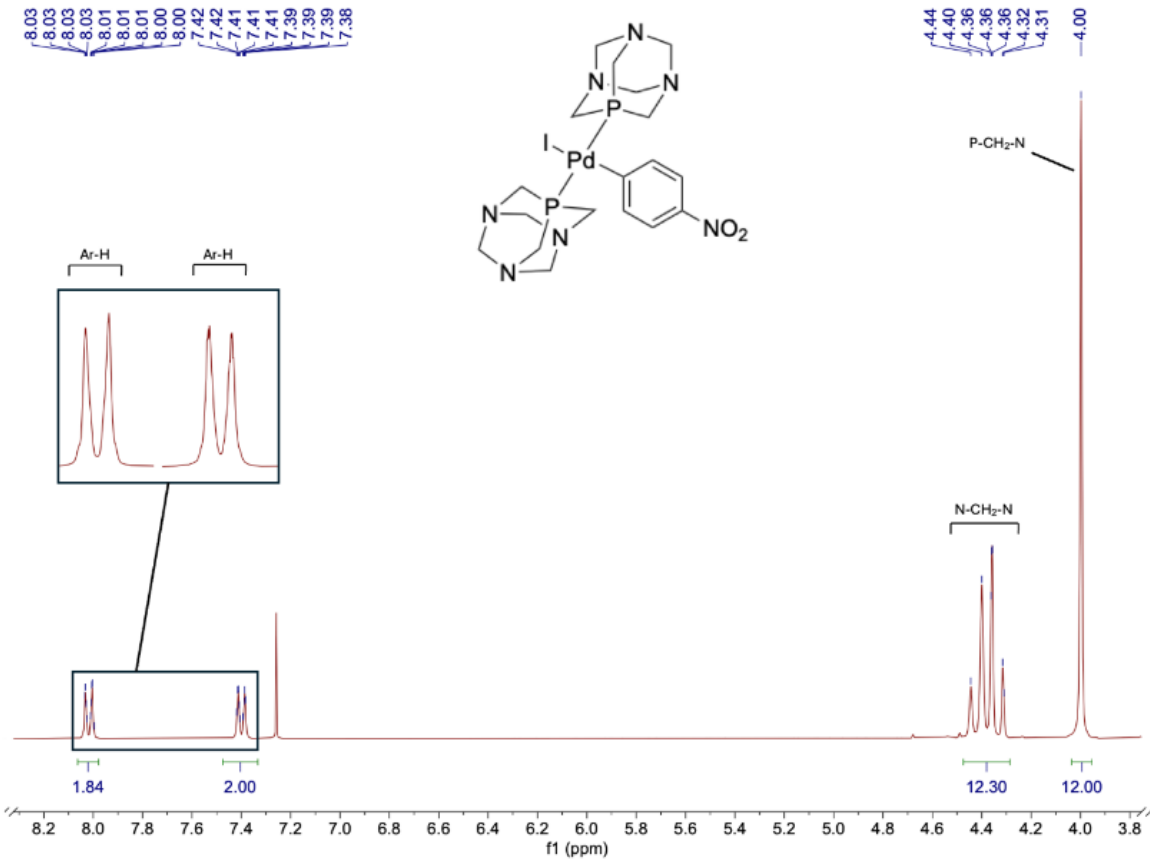

Figure S33. ^{1}H NMR spectrum of **7a** in $CDCl_3$ at 298 K.

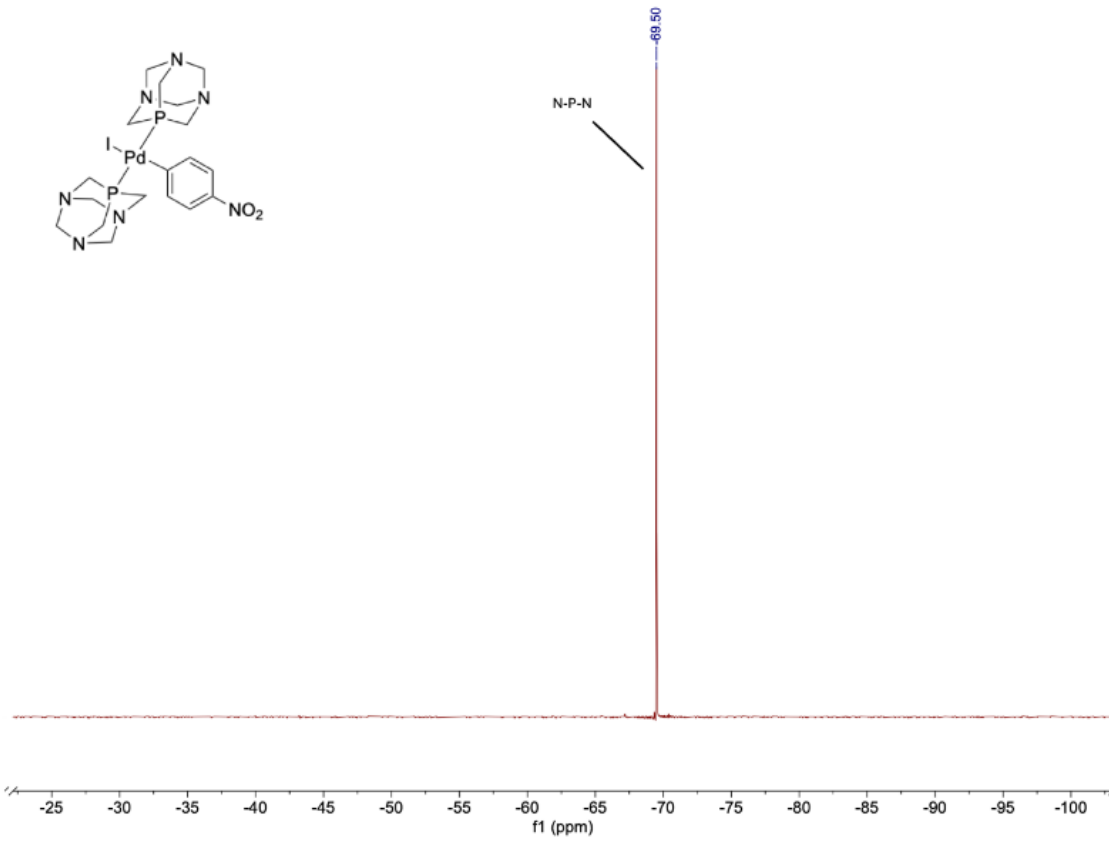

Figure S34. $^{31}P\{^{1}H\}$ NMR spectrum of **7a** in $CDCl_3$ at 298 K

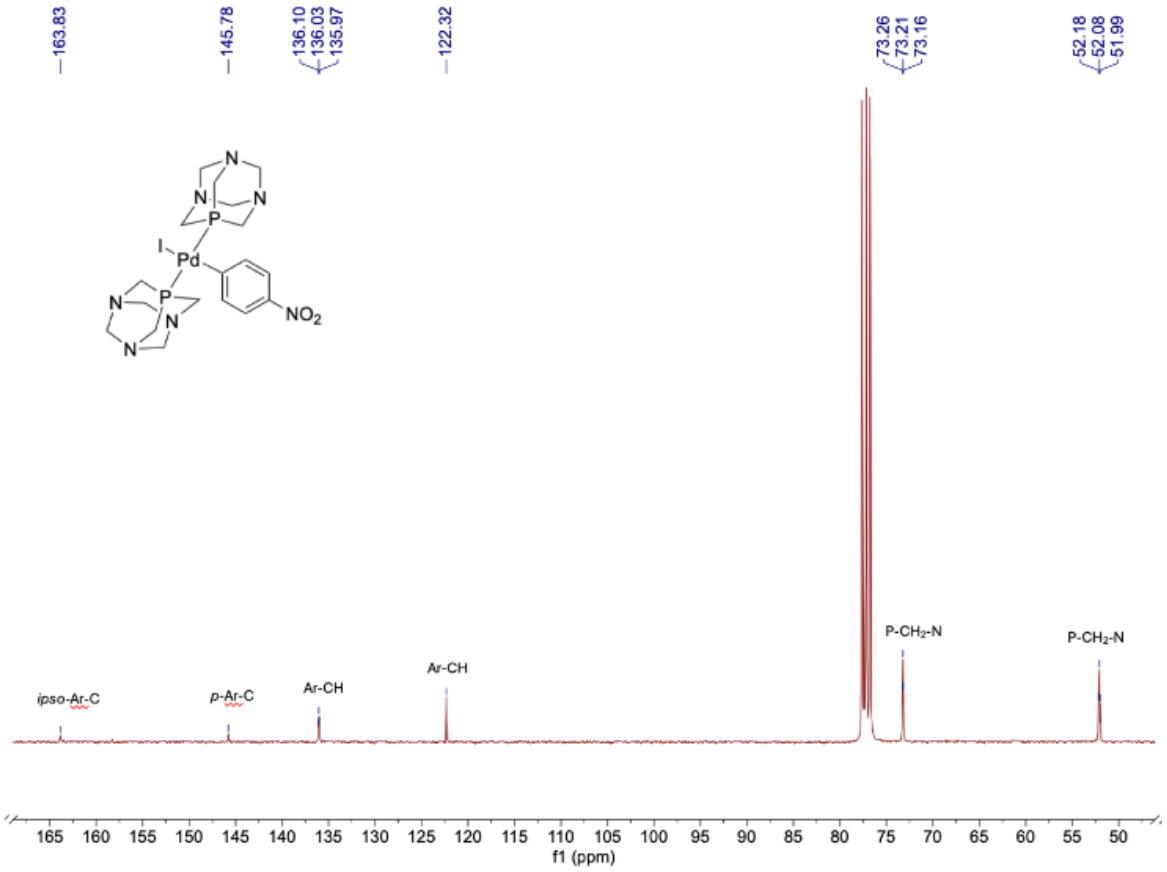

Figure S35. $^{13}C\{^{1}H\}$ NMR spectrum of **7a** in $CDCl_3$ at 298 K

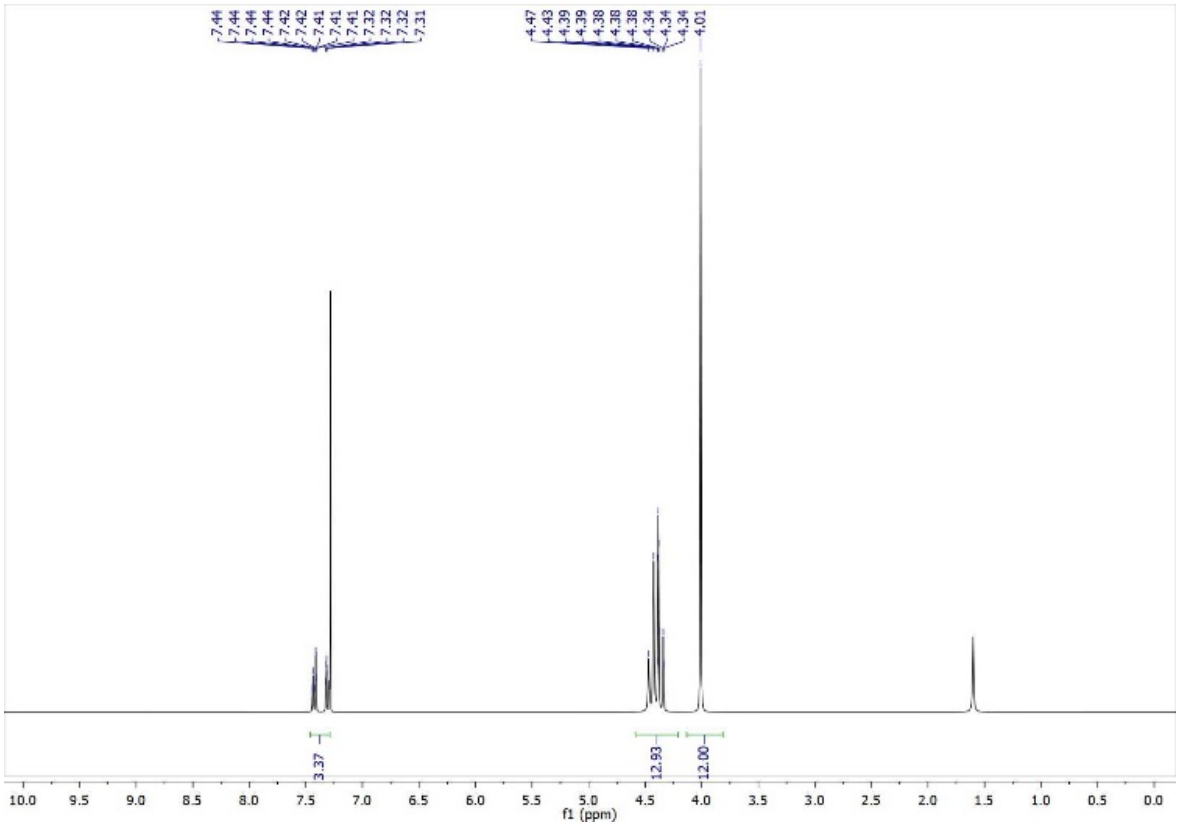

Figure S36. ^{1}H NMR spectrum of **7a** in $CDCl_3$ at 298 K.

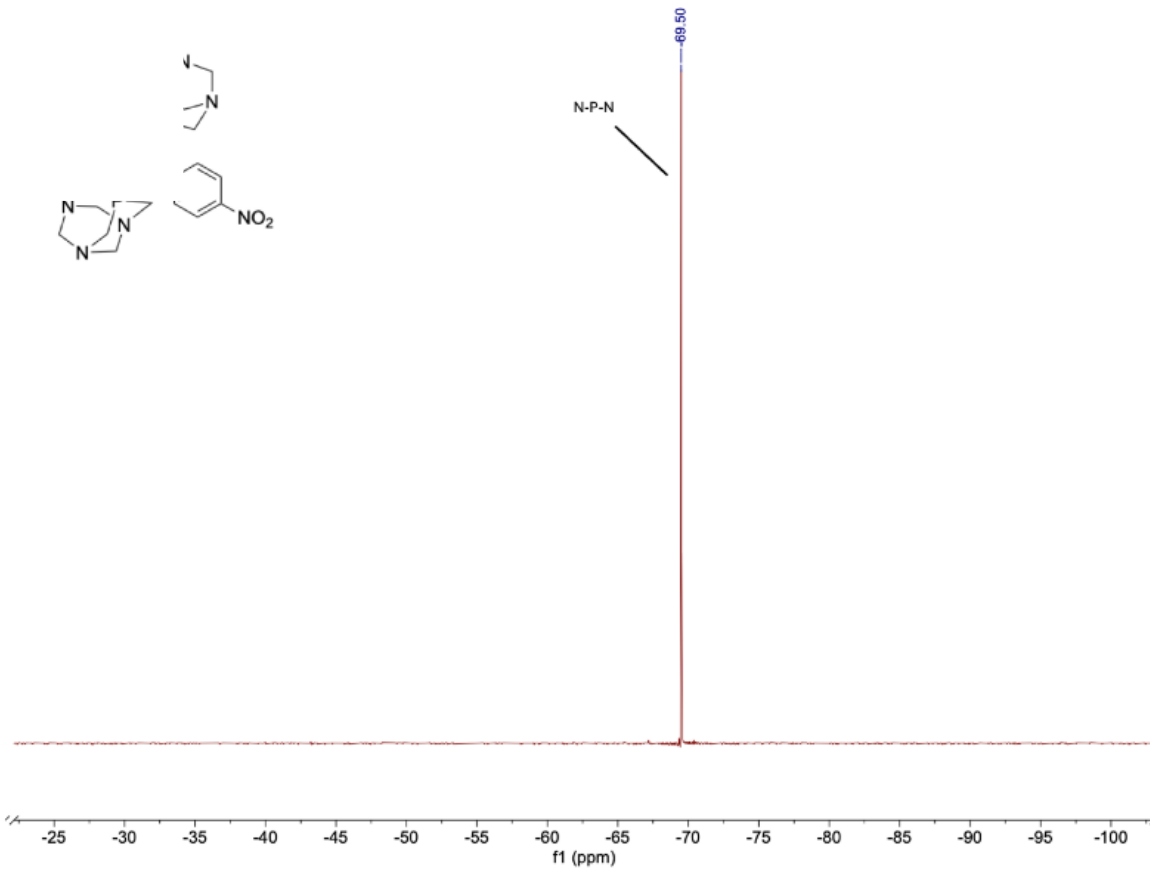

Figure S37. $^{31}P\{^{1}H\}$ NMR spectrum of **7a** in $CDCl_3$ at 298 K

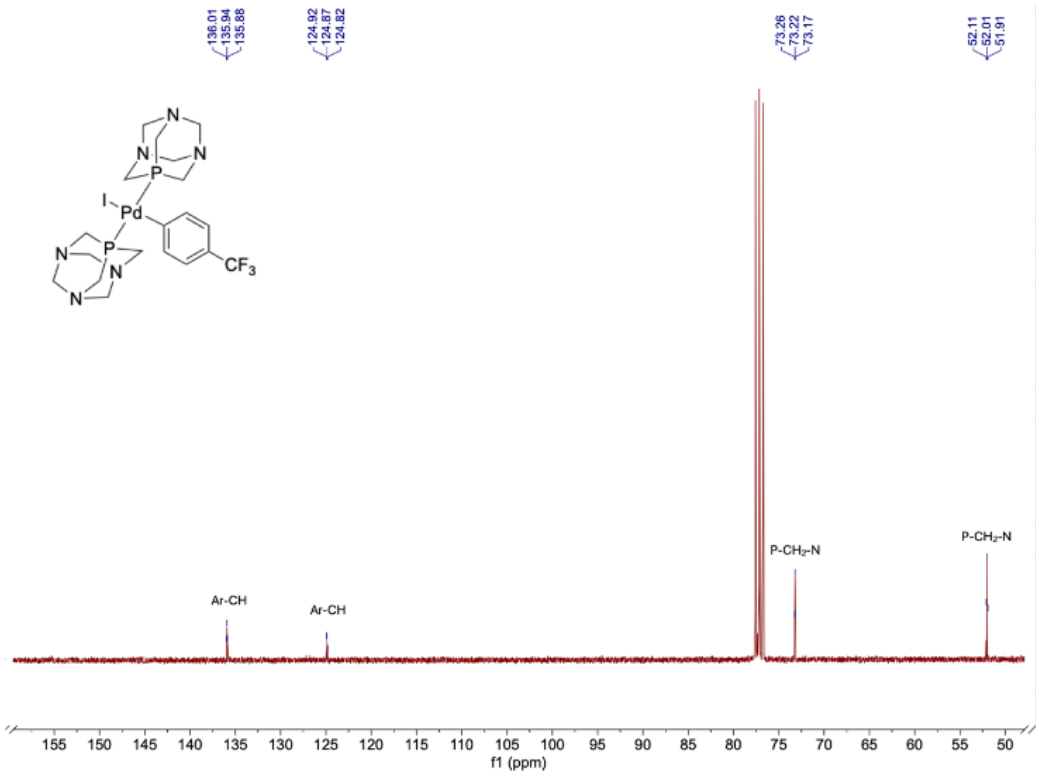

Figure S38. $^{13}C\{^{1}H\}$ NMR spectrum of **7a** in CD_3CN at 298 K

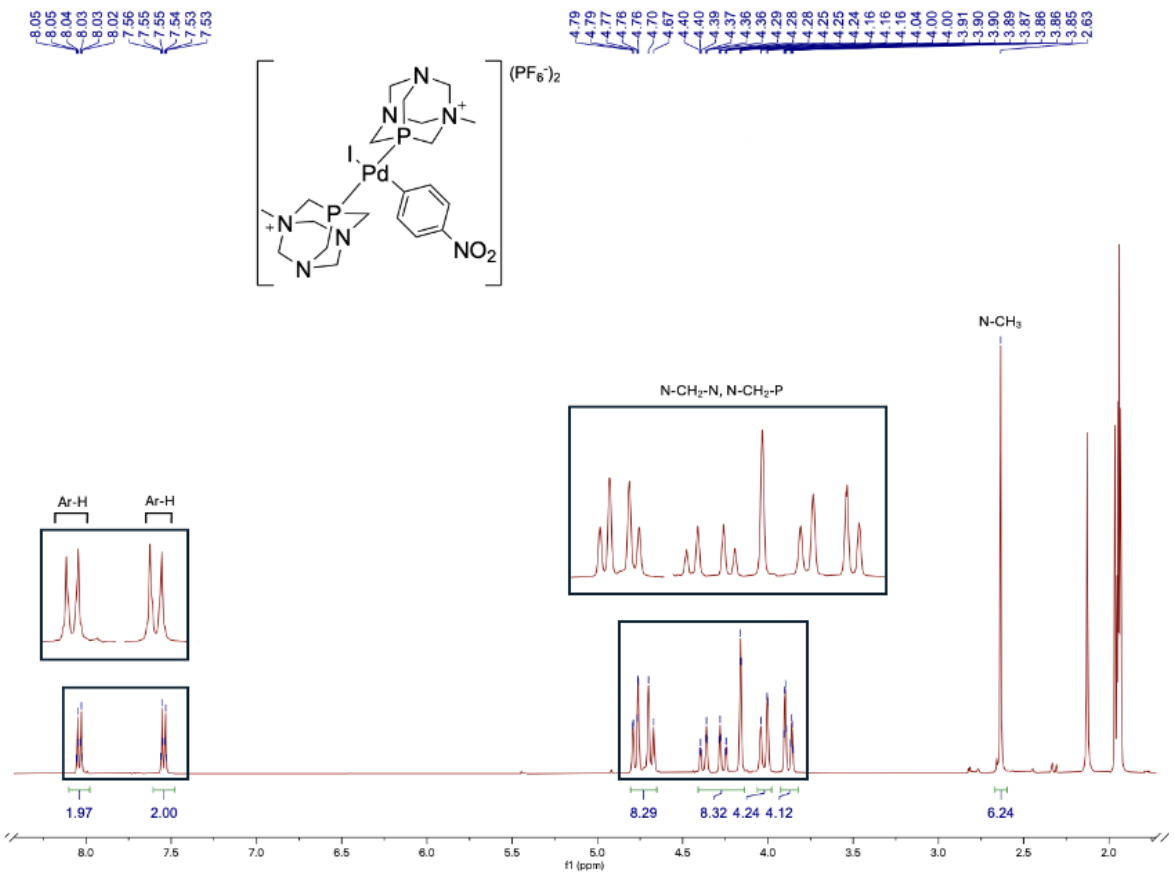

Figure S39. ^{1}H NMR spectrum of **7b** in CD_3CN at 298 K.

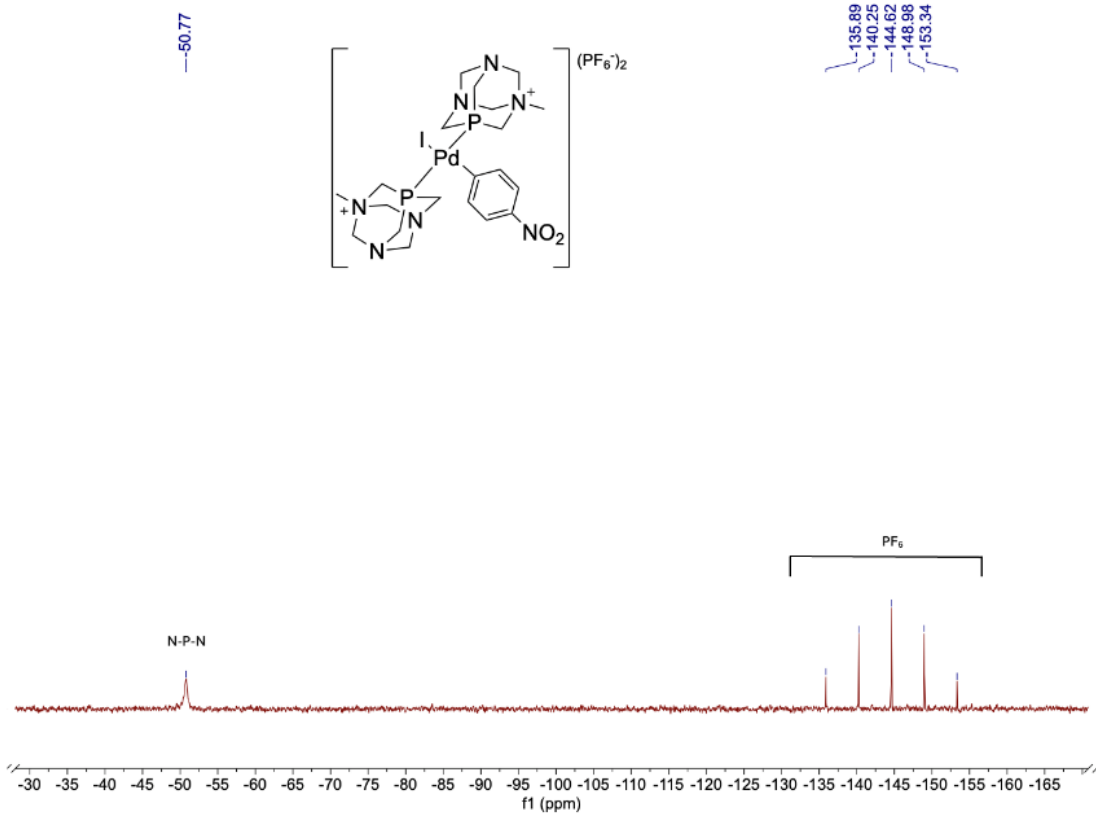

Figure S40. $^{31}P\{^{1}H\}$ NMR spectrum of **7b** in CD_3CN at 298 K

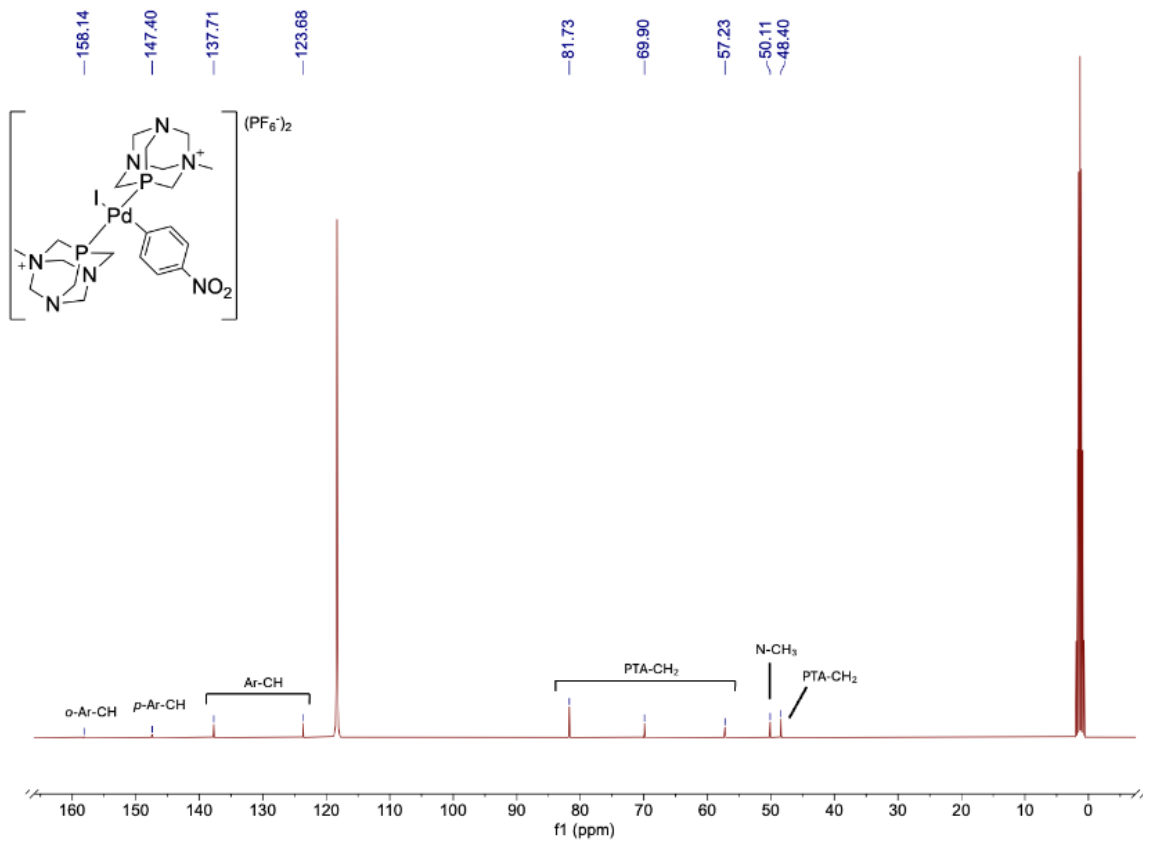

Figure S41. $^{13}C\{^{1}H\}$ NMR spectrum of **7b** in CD_3CN at 298 K

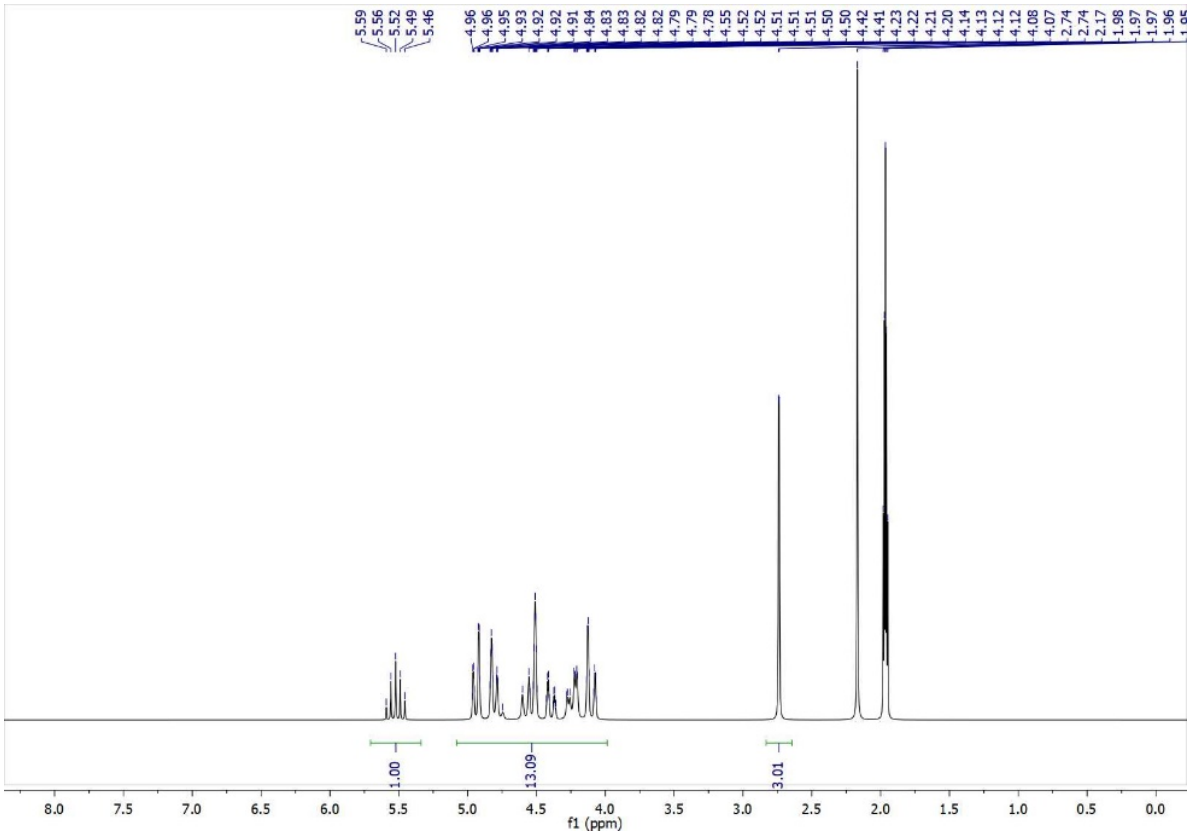

Figure S42. ^{1}H NMR spectrum of **10b** in CD_3CN at 298 K.

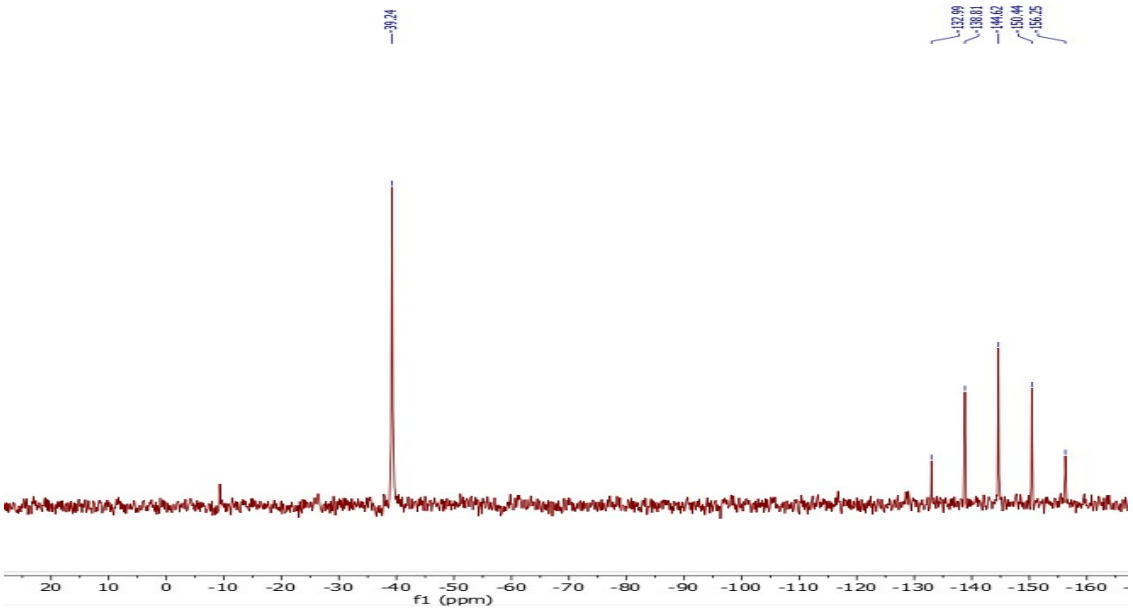

Figure S43. $^{31}P\{^{1}H\}$ NMR spectrum of **10b** in CD_3CN at 298 K

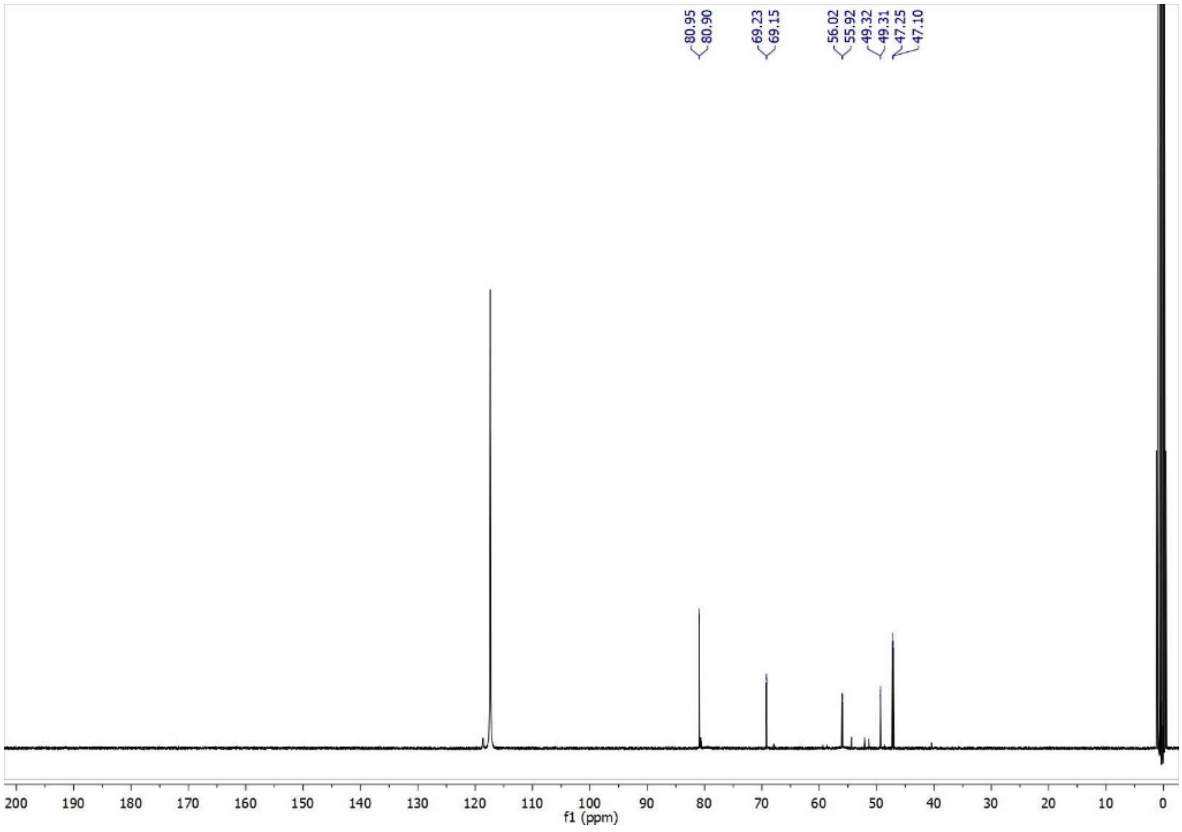

Figure S44. $^{13}C\{^{1}H\}$ NMR spectrum of **10b** in CD_3CN at 298 K

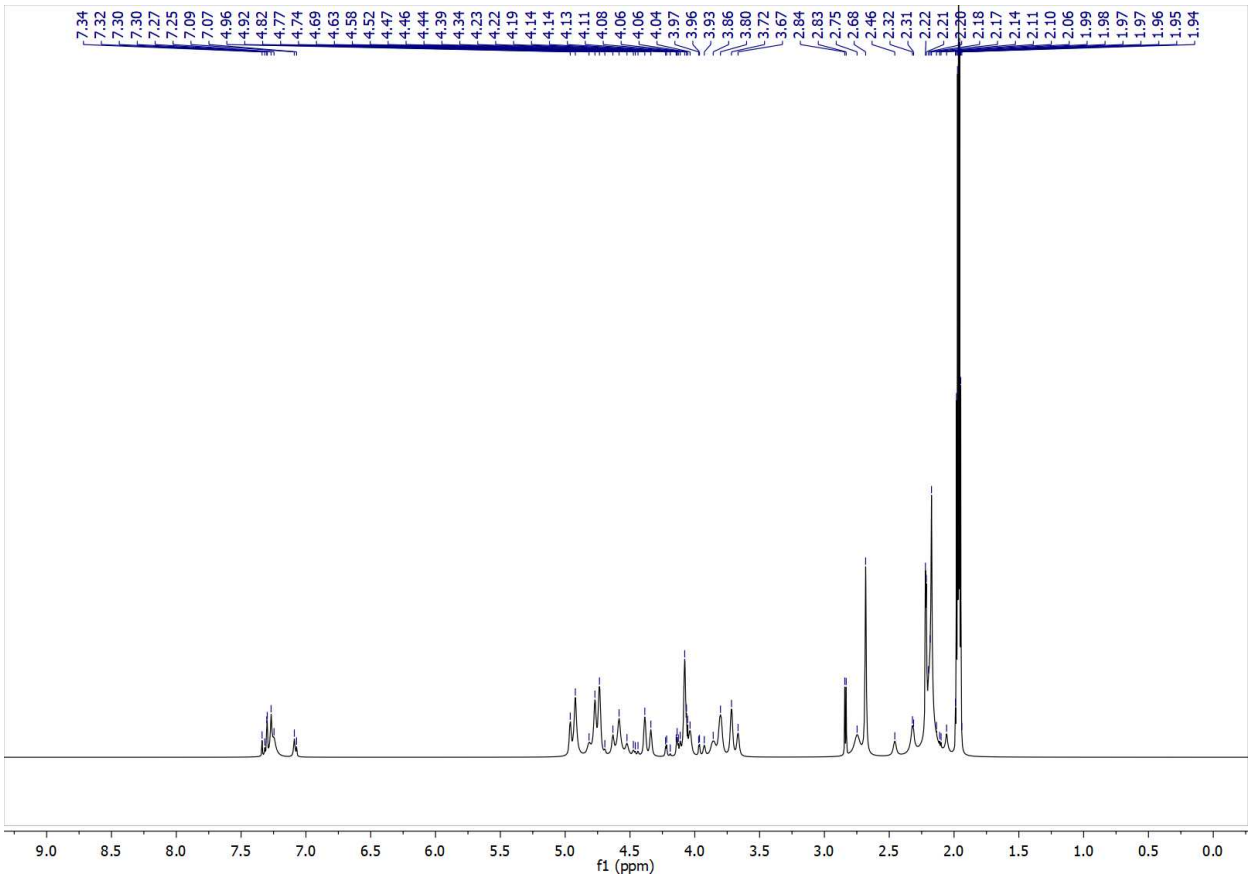

Figure S45. ^{1}H NMR spectrum of **12b** in CD_3CN at 298 K.

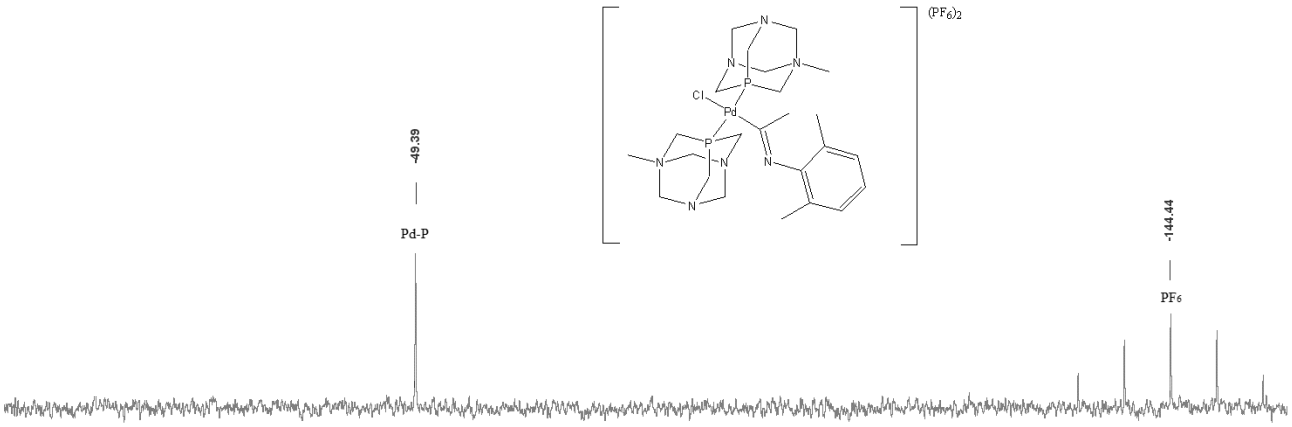

Figure S46. $^{31}P\{^{1}H\}$ NMR spectrum of **12b** in CD_3CN at 298 K

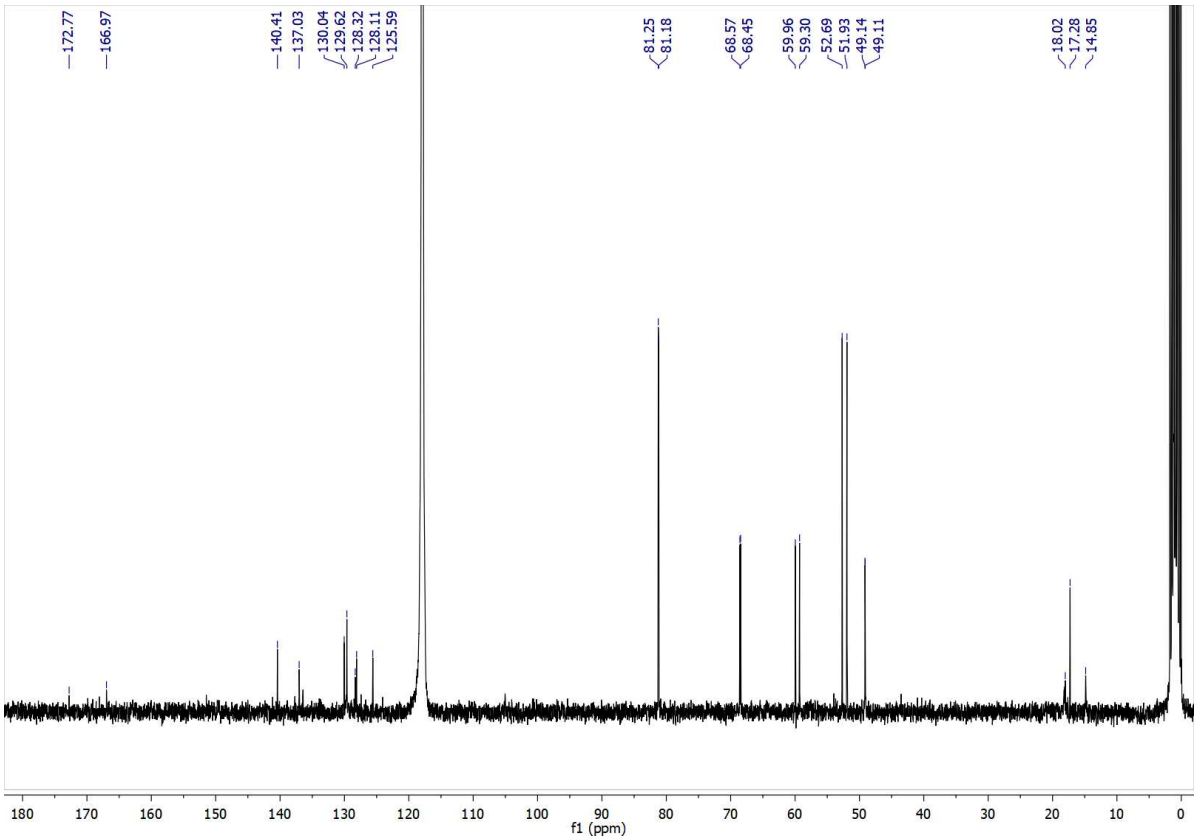

Figure S47. $^{13}C\{^{1}H\}$ NMR spectrum of **12b** in CD_3CN at 298 K

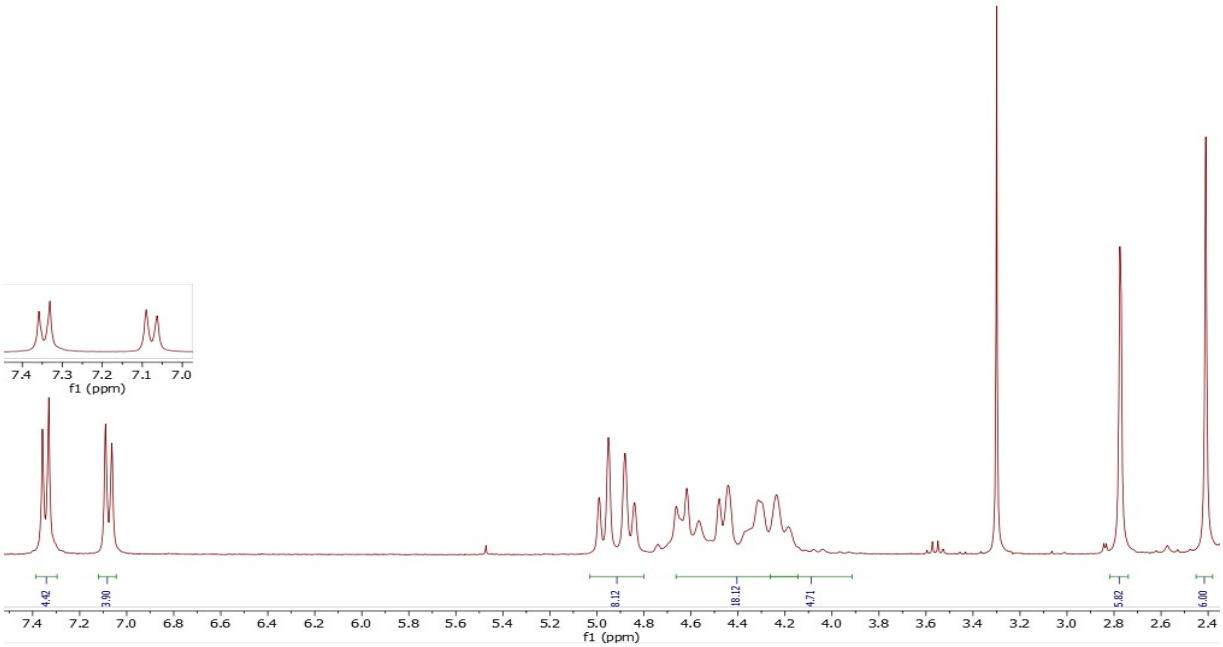

Figure S48. ^{1}H NMR spectrum of **14b** in CD_3CN at 298 K.

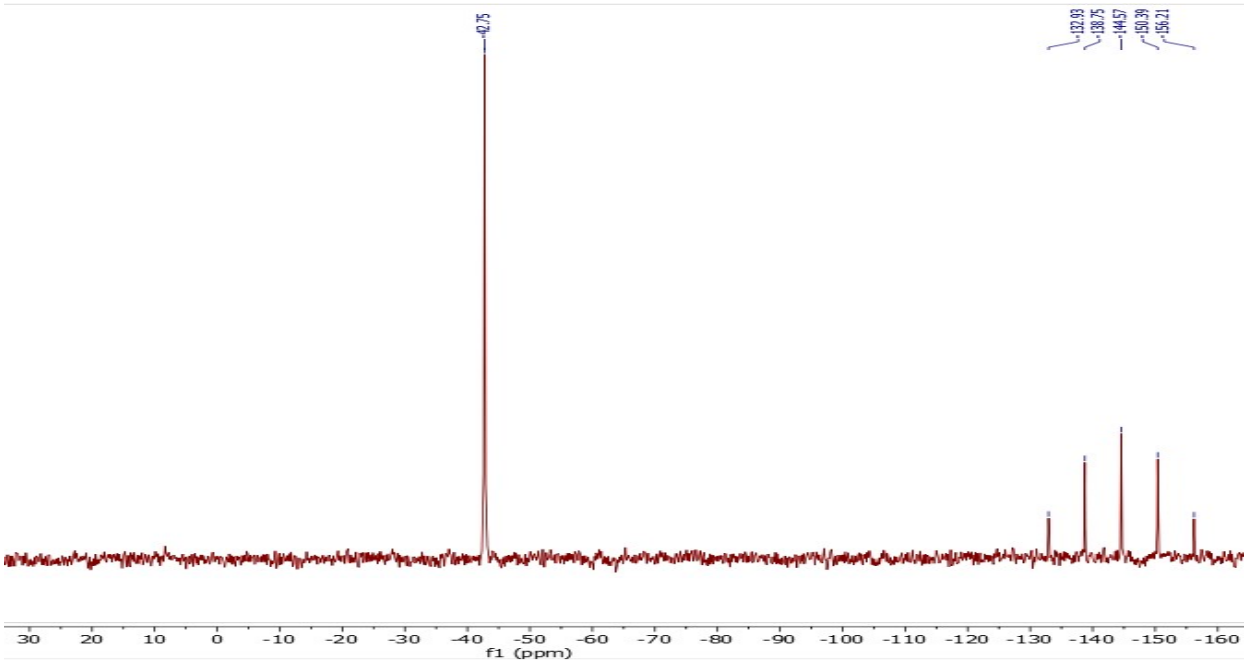

Figure S49. $^{31}P\{^{1}H\}$ NMR spectrum of **14b** in CD_3CN at 298 K

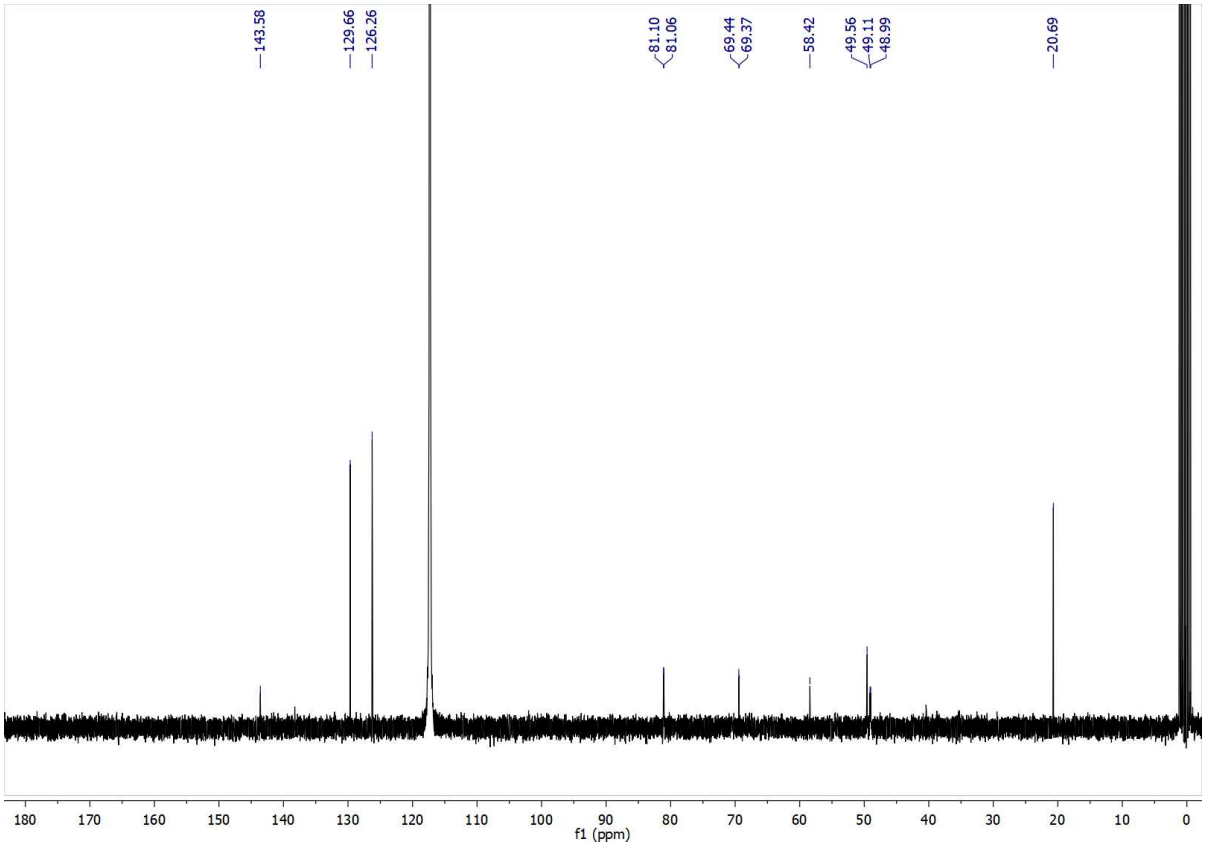

Figure S50. $^{13}C\{^{1}H\}$ NMR spectrum of **14b** in CD_3CN at 298 K

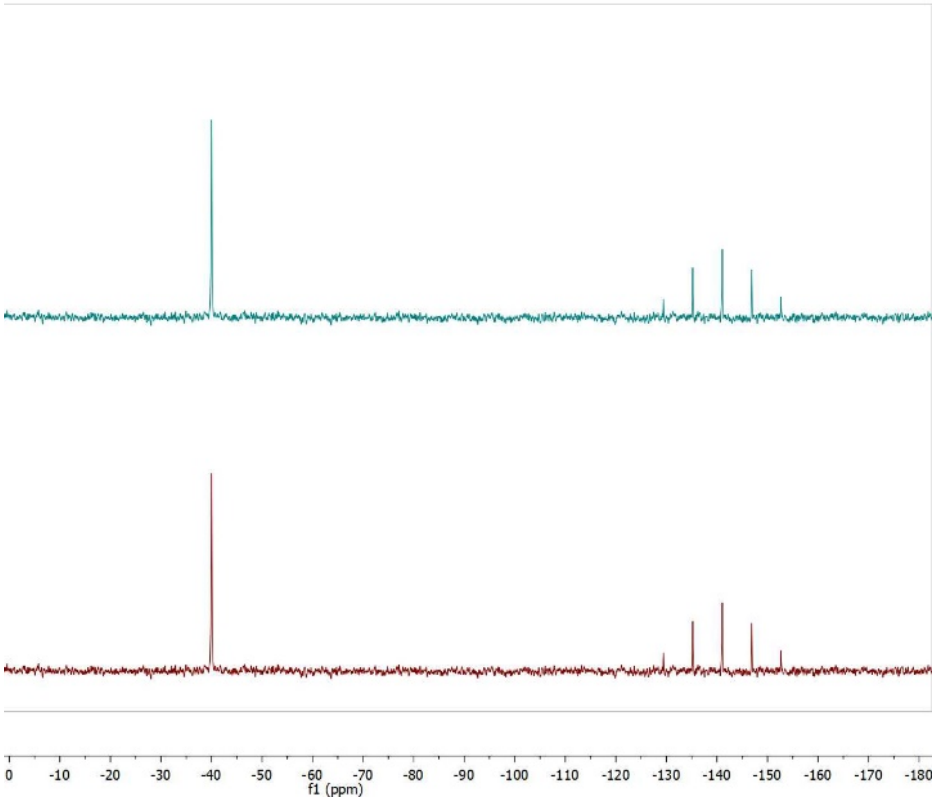

Figure S51: $^{31}P\{^{1}H\}$ NMR of **3b** in culture medium/DMSO-d_6 (1:2) at 0 (red) and 48h (green).

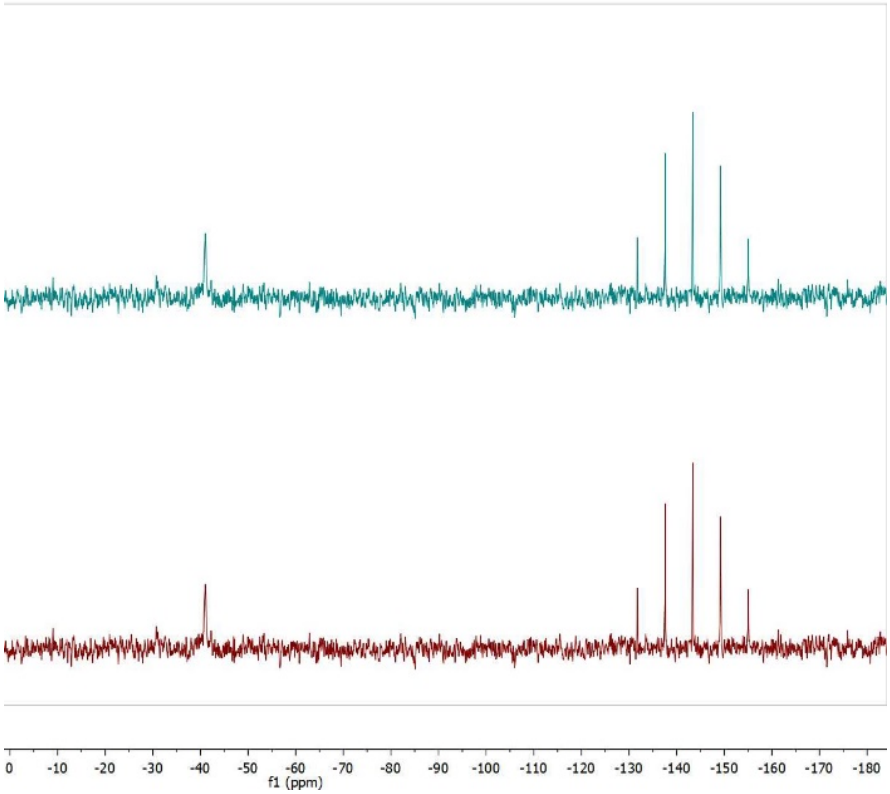

Figure S52: $^{31}P\{^{1}H\}$ NMR of **3c** in culture medium/DMSO-d_6 (1:2) at 0 (red) and 48h (green).

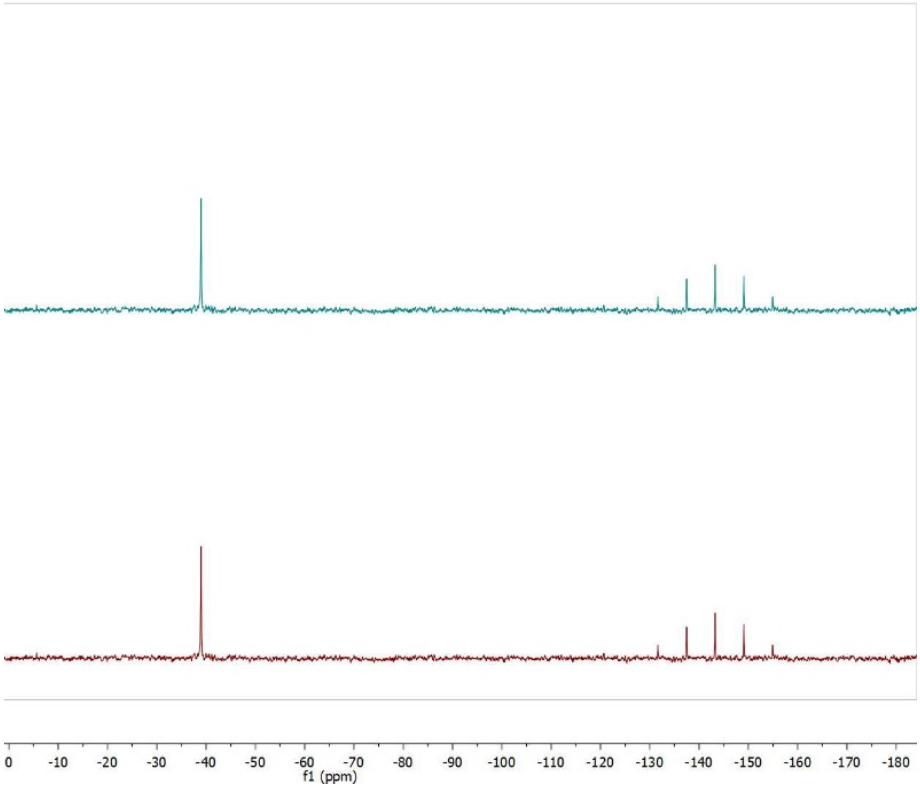

Figure S53: $^{31}P\{^{1}H\}$ NMR of **3d** in culture medium/DMSO-d_6 (1:2) at 0 (red) and 48h (green).

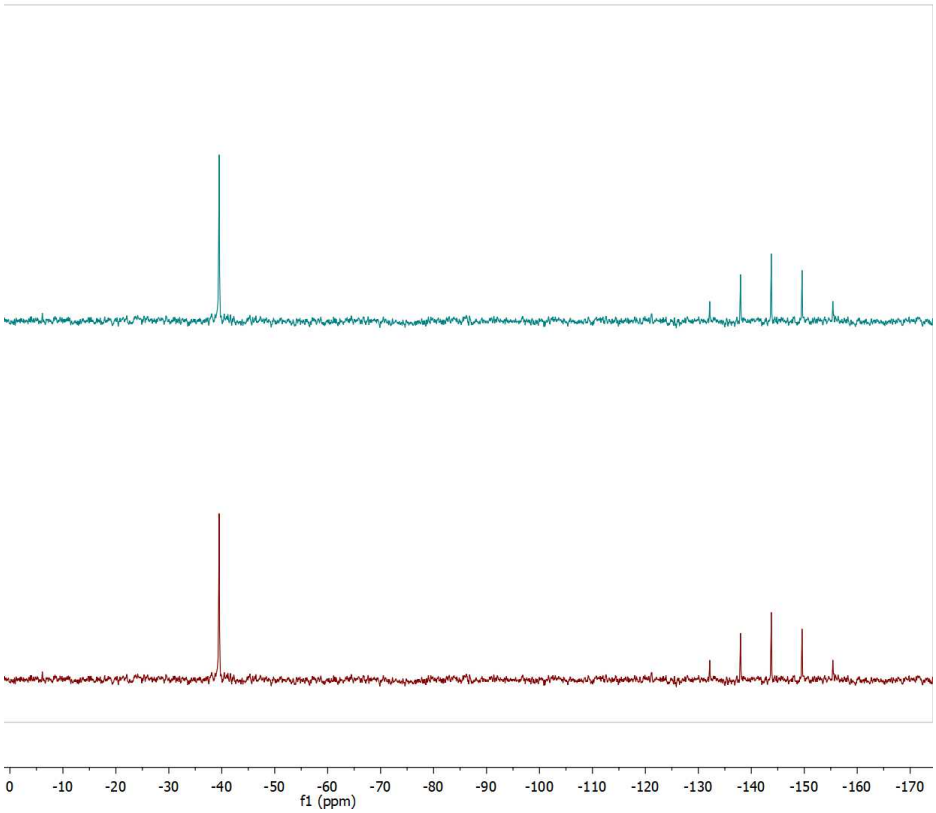

Figure S54: $^{31}P\{^{1}H\}$ NMR of **3e** in culture medium/DMSO-d_6 (1:2) at 0 (red) and 48h (green).

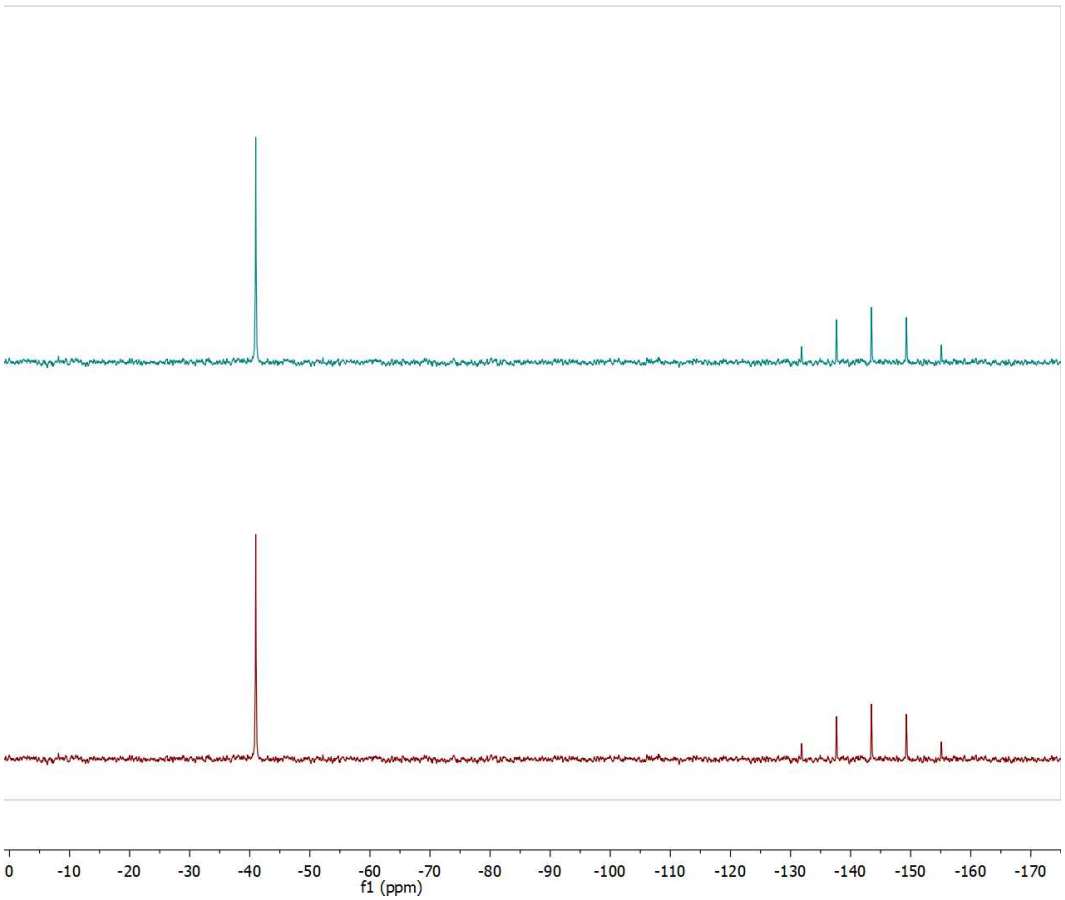

Figure S55: $^{31}P\{^{1}H\}$ NMR of **4b** in culture medium/DMSO-d_6 (1:2) at 0 (red) and 48h (green).

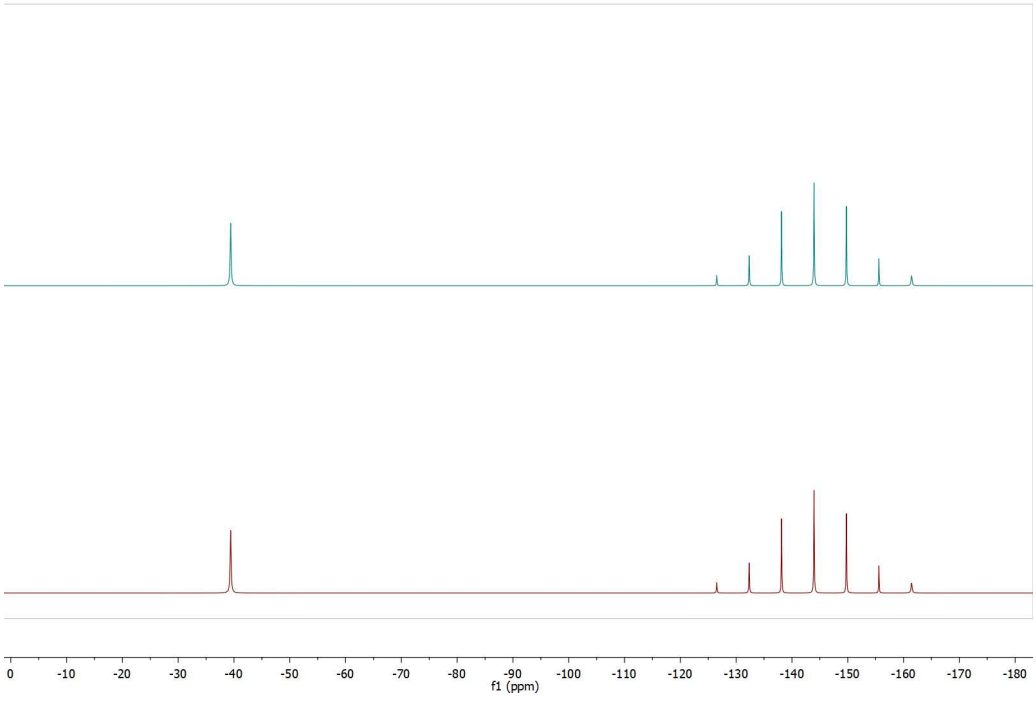

Figure S56: $^{31}P\{^{1}H\}$ NMR of **4c** in culture medium/DMSO-d_6 (1:2) at 0 (red) and 48h (green).

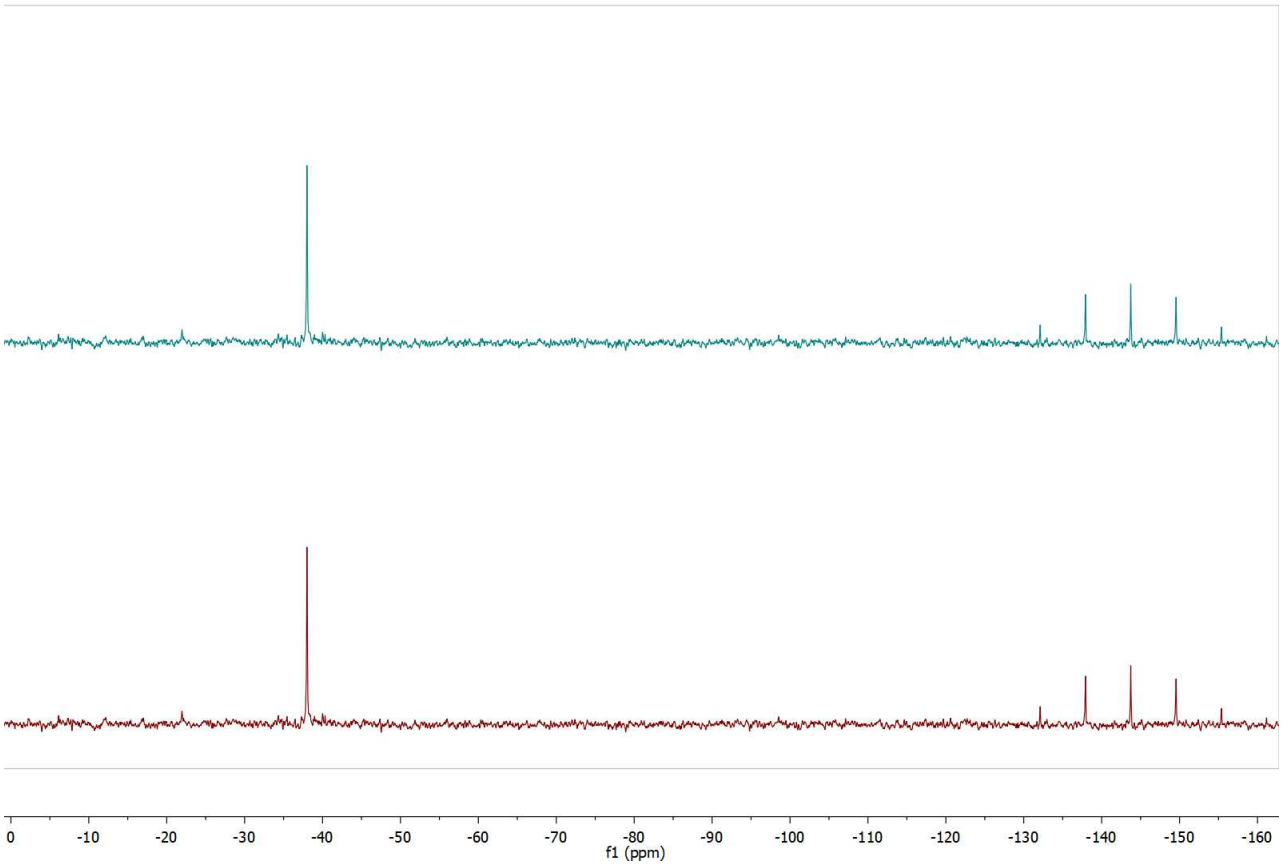

Figure S57: $^{31}P\{^{1}H\}$ NMR of **4d** in culture medium/DMSO-d_6 (1:2) at 0 (red) and 48h (green).

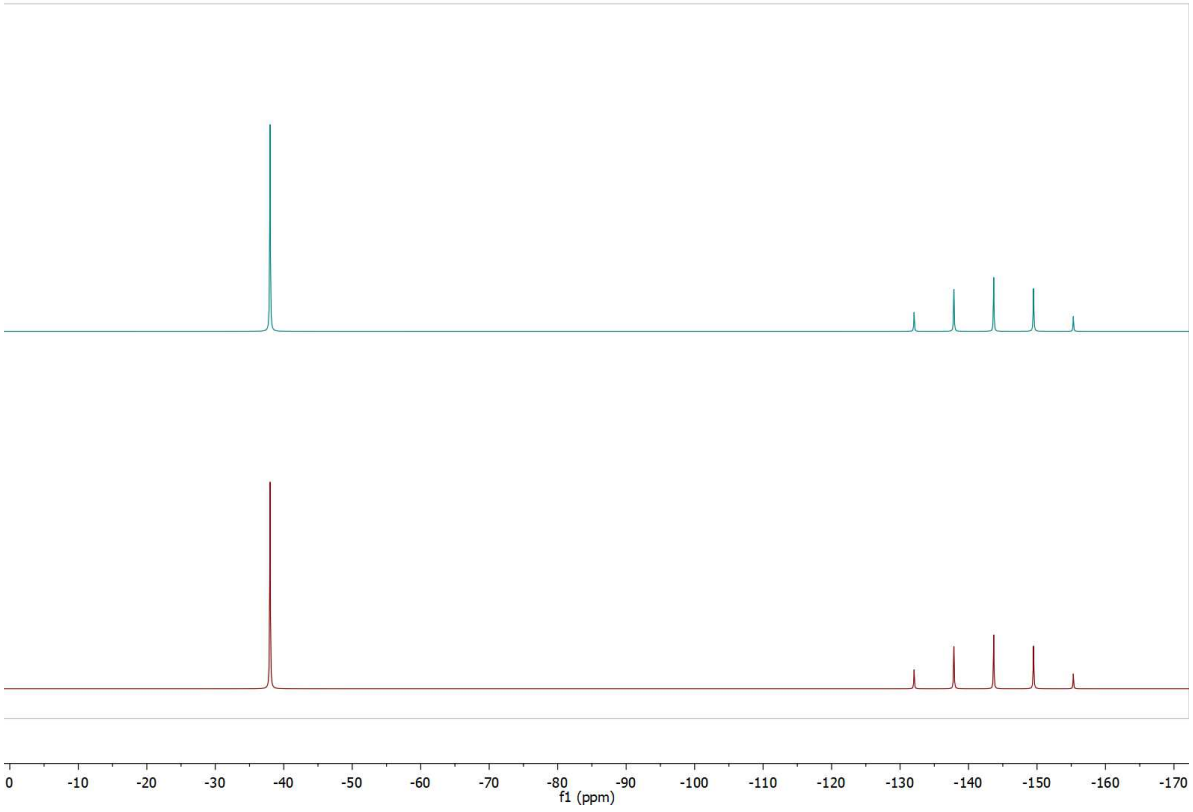

Figure S58: $^{31}P\{^{1}H\}$ NMR of **4e** in culture medium/DMSO-d_6 (1:2) at 0 (red) and 48h (green).

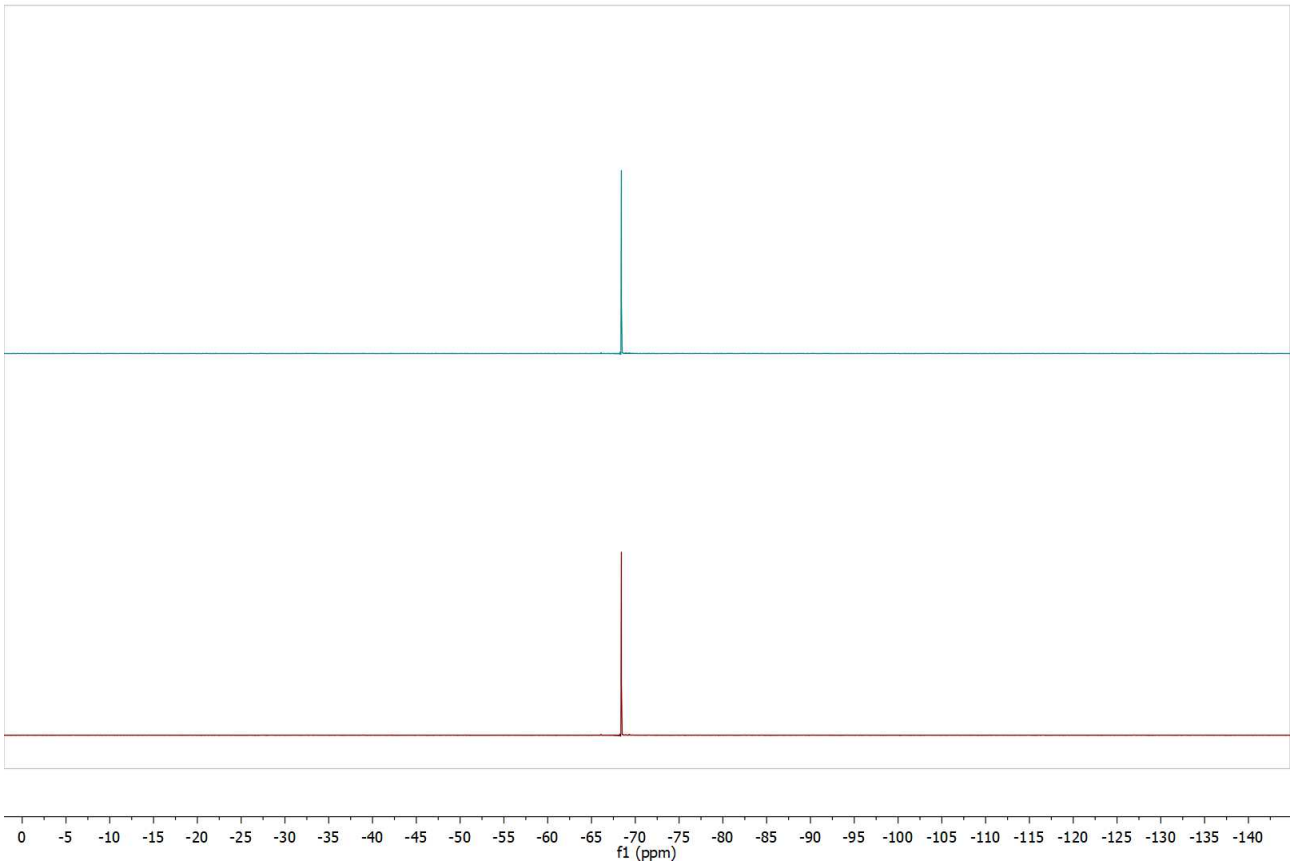

Figure S59: $^{31}P\{^{1}H\}$ NMR of **8a** in culture medium/DMSO-d_6 (1:2) at 0 (red) and 48h (green).

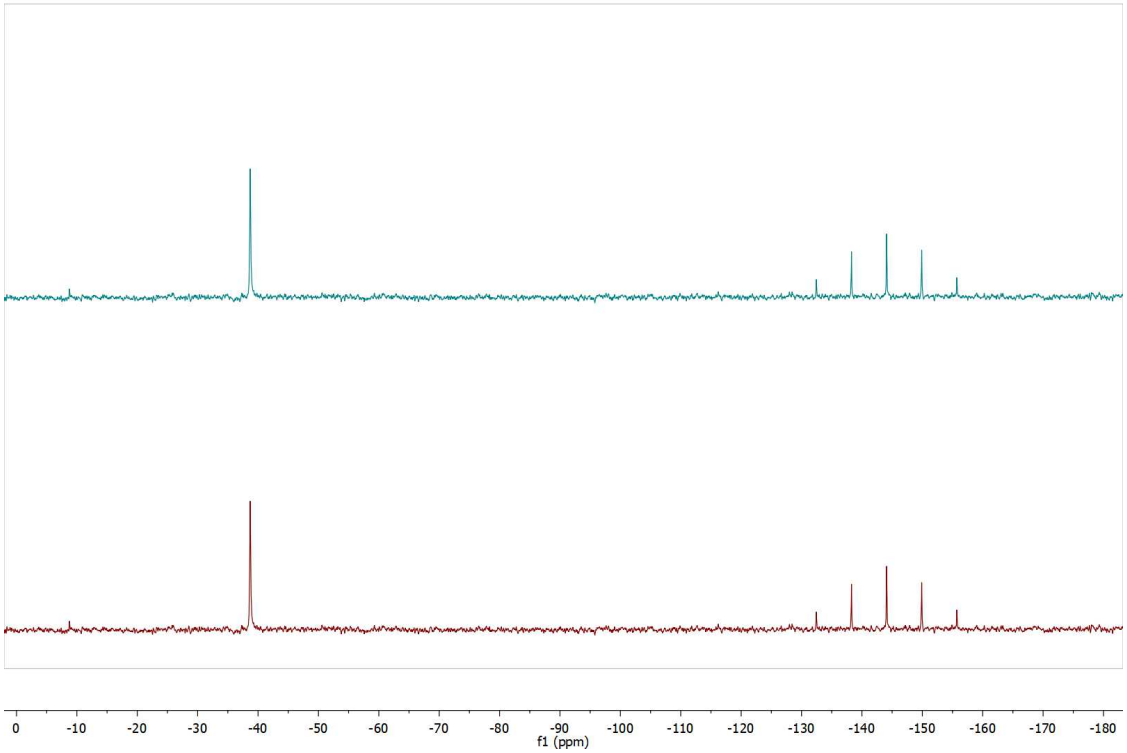

Figure S60: $^{31}P\{^{1}H\}$ NMR of **10b** in culture medium/DMSO-d_6 (1:2) at 0 (red) and 48h (green).

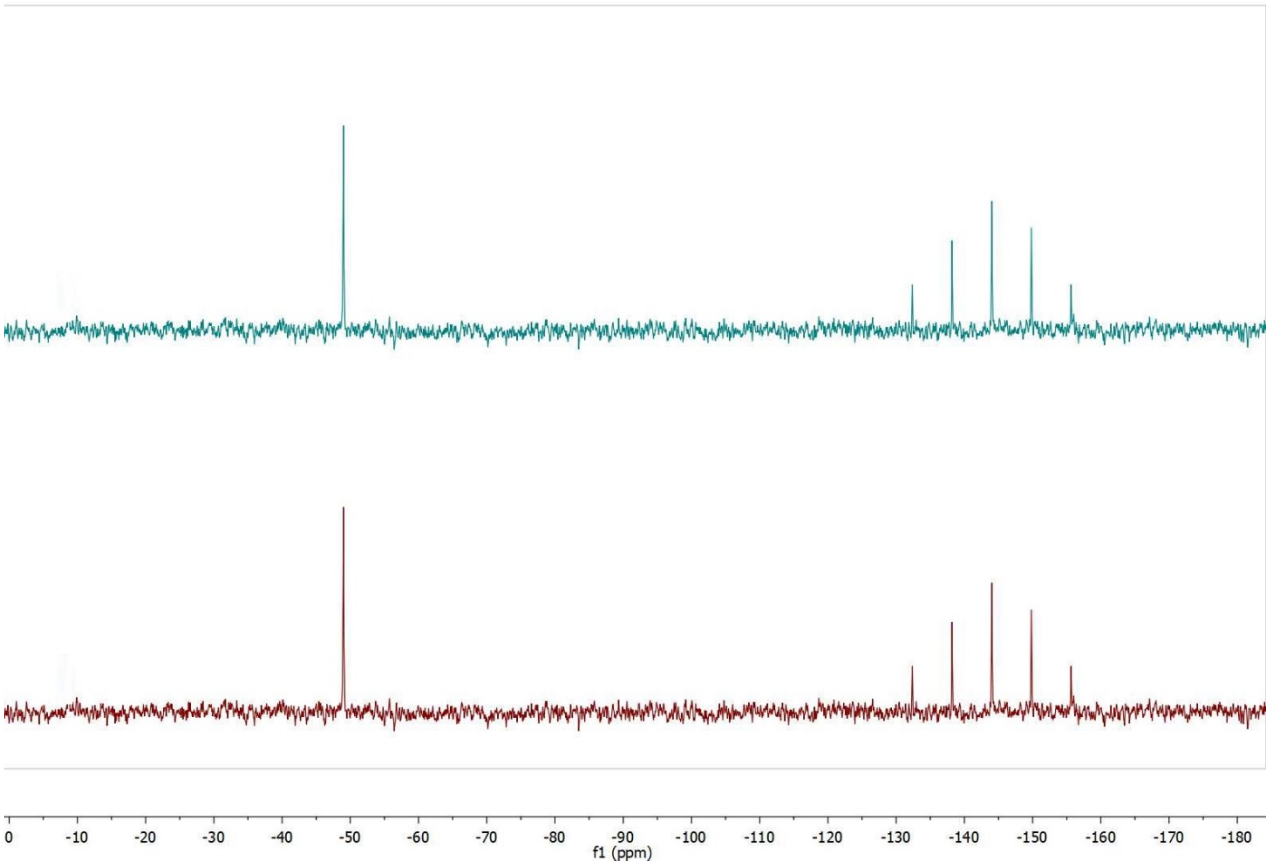

Figure S61: $^{31}P\{^{1}H\}$ NMR of **12b** in culture medium/DMSO-d_6 (1:2) at 0 (red) and 48h (green).

X-RAY DIFRACTION ANALYSIS

Table S1. Crystallographic data.

Compound	**8a**	**7a**
CCDC Deposition N.	2411281	2411282
Formula	$PdC_{19}H_{28}F_3IN_6P_2$	$PdC_{18}H_{28}IN_7O_2P_2$
M/g·mol^{-1}	692.71	669.71
Space group	*C* 2/*c*	*P* -1
Crystal system	Monoclinic	Triclinic
a/Å	18.983(4)	10.593(2)
b/Å	12.971(3)	10.717(2)
c/Å	10.549(2)	11.282(2)
α/°	90	88.76(3)
β/°	112.82(3)	74.42(3)
γ/°	90	74.02(3)
V/Å^3	2394.1(10)	1184.3(5)
Z	4	2
T/K	100(2)	100(2)
D_c/g·cm^{-3}	1.922	1.878
F(000)	1360	660
μ/mm^{-1}	1.532	1.539
Measured Reflections	26947	54031
Unique Reflections	5270	10319
R_{int}	0.0509	0.0459
Obs. Refl.ns [I≥2σ(I)]	4350	9784
θ_{min}- θ_{max}/°	1.70 – 31.06	1.73 – 31.11
hkl ranges	-30,30; -21,21; -17,17	-17,17; -17,17; -18,18
R(F^2) (Obs.Refl.ns)	0.0435	0.0288
wR(F^2) (All Refl.ns)	0.1283	0.0721
No. Variables	161	280
Goodness of fit	1.208	1.067
$\Delta\rho_{max}$; $\Delta\rho_{min}$/e·Å^{-3}	1.86; -2.10	1.78; -2.27

Table S2. Selected palladium distances and angles for **8a** at 100 K.

8a (100 K) - $PdC_{19}H_{28}F_3IN_6P_2$

Distances	(Å)	**Angles**	(°)
Pd_1-C4_4	2.023(4)	I_2-Pd_1- P1_3	94.40(2)
Pd_1-I_2	2.668(1)	P1_3-Pd_1-C4_4	85.60(2)
Pd_1-P1_3	2.292(1)	C4_4-Pd_1-P1_3	85.60(2)
Pd_1-P1_3	2.292(1)	P1_3-Pd_1-I_2	94.40(2)
		Pd.- Phenyl	83.17(8)
		Average Planes[a]	

[a]Angle between the mean metal coordination plane and the phenyl ligand core average plane.

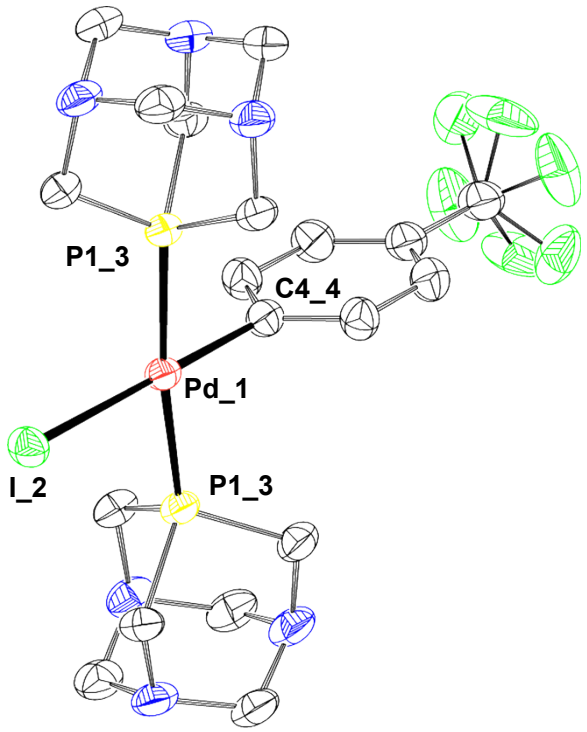

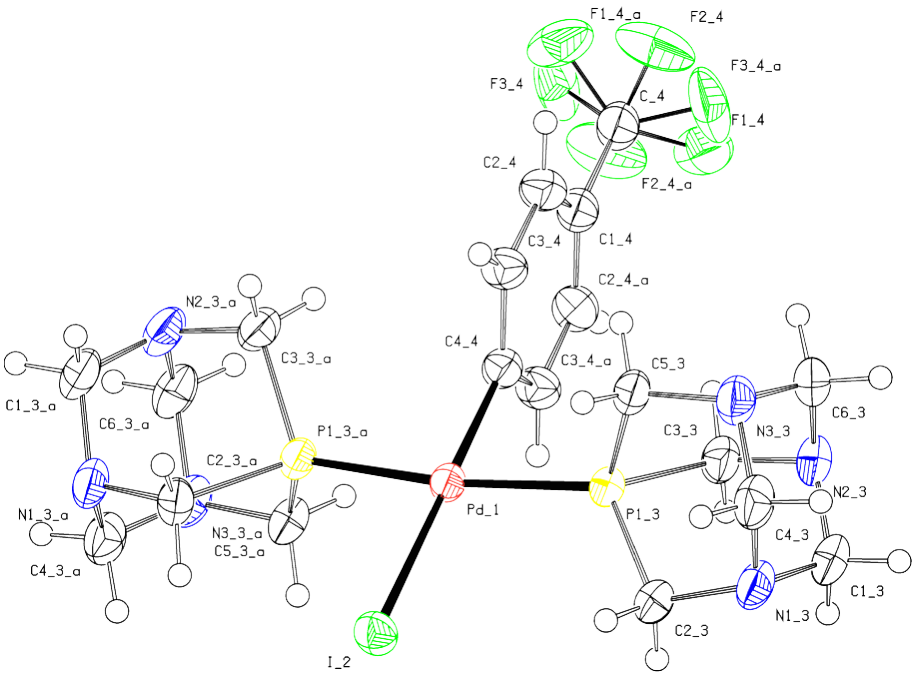

Table S3. Selected palladium distances and angles for **7a** at 100 K.

7a (100 K) - $PdC_{18}H_{28}IN_7O_2P_2$

Distances	(Å)	**Angles**	(°)
Pd_1-C3_4	2.008(1)	I_2-Pd_1- P1_5	89.61(1)
Pd_1-I_2	2.667(1)	P1_5-Pd_1-C3_4	88.22(4)
Pd_1-P1_3	2.290(1)	C3_4-Pd_1-P1_3	87.01(4)
Pd_1-P1_5	2.290(1)	P1_3-Pd_1-I_2	95.12(1)
		Pd.- Phenyl	89.99(4)
		Average Planes[a]	

[a]Angle between the mean metal coordination plane and the phenyl ligand core average plane.

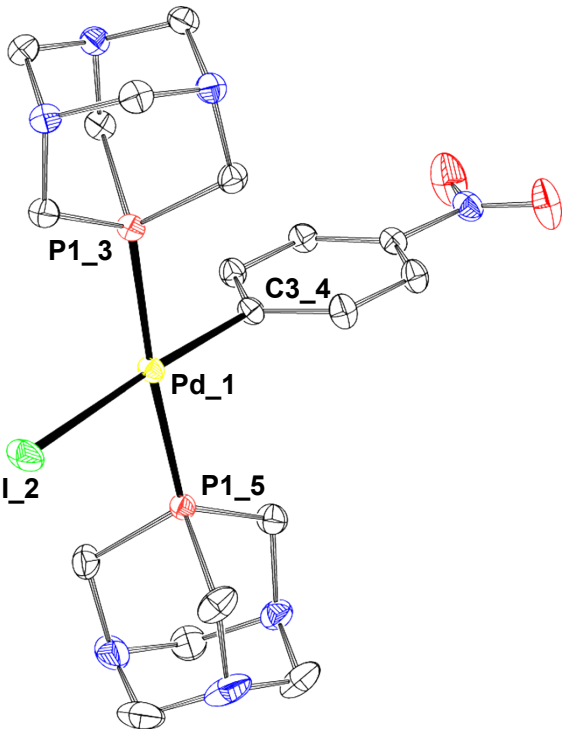

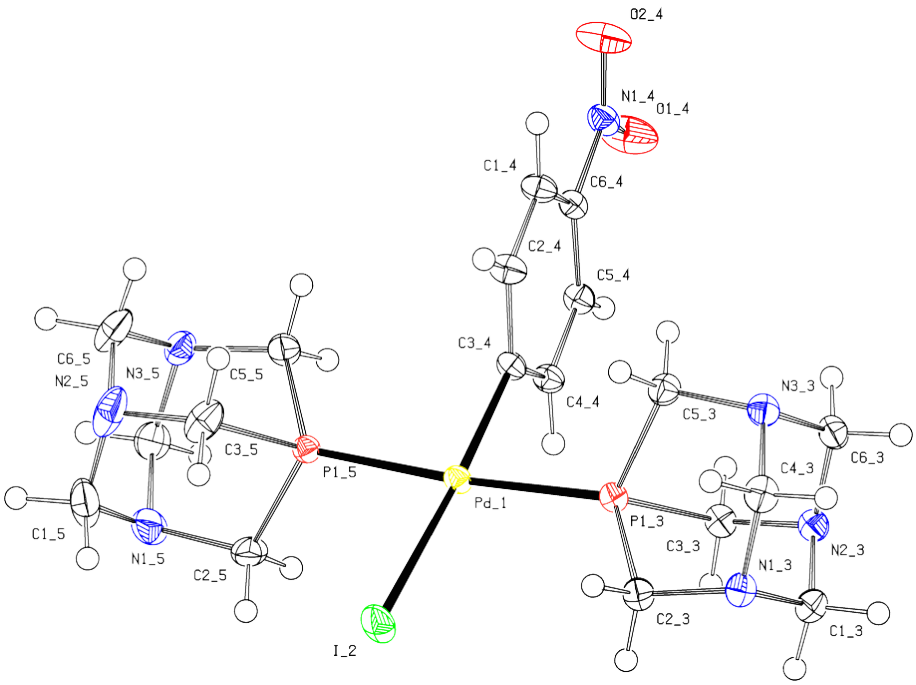

Computational details

Electronic energies (Hartree), imaginary frequency (cm^{-1}) and cartesian coordinates (Å) of compound **8a**

E= -12.12796834 a.u.

NIMAG=0

I	6.425710000	-1.024255000	7.287497000
N	11.015093000	0.856786000	5.665034000
P	8.761932000	1.726683000	7.092598000
N	11.247448000	3.021036000	6.873396000
C	9.799222000	3.308348000	6.990747000
H	9.471216000	3.897576000	6.126823000
H	9.617070000	3.915029000	7.885103000
C	9.538357000	0.841706000	5.607534000
H	9.169200000	-0.189006000	5.593859000
H	9.201008000	1.332415000	4.686761000
C	11.749774000	2.264997000	8.047297000
H	11.496159000	2.812568000	8.962042000
H	12.841536000	2.204230000	7.966442000
C	11.521216000	0.167891000	6.879605000
H	12.610745000	0.084739000	6.790004000
H	11.092963000	-0.838819000	6.925354000
N	11.221180000	0.881922000	8.146888000
C	9.774032000	0.870747000	8.446927000
H	9.592398000	1.380773000	9.400517000
H	9.414125000	-0.158991000	8.542178000
C	11.550609000	2.240657000	5.648201000
H	12.640863000	2.179707000	5.549150000
H	11.148823000	2.770143000	4.776935000
Pd	6.420707000	1.752102000	7.290990000
C	3.070587000	0.858752000	6.133790000
H	3.434161000	-0.169605000	6.037607000
H	0.199140000	2.154993000	9.032812000
F	7.745241000	8.647064000	7.188555000
C	6.406413000	6.661128000	7.301521000

C	6.514630000	5.951073000	8.505198000
H	6.589963000	6.487798000	9.447846000
C	6.517905000	4.551247000	8.496372000
H	6.598708000	4.029094000	9.448286000
C	6.417184000	3.822758000	7.294887000
H	1.689118000	2.750078000	9.805460000
C	1.289166000	2.219910000	8.933759000
H	3.250376000	1.370235000	5.180631000
C	6.307391000	5.955899000	6.094205000
H	6.220920000	6.496420000	5.154676000
C	6.311768000	4.556057000	6.096716000
H	6.229041000	4.037733000	5.142879000
N	1.829629000	0.838031000	8.915703000
P	4.079722000	1.717060000	7.488816000
N	1.589422000	3.002536000	7.709184000
C	3.036707000	3.294850000	7.592015000
H	3.362764000	3.884457000	8.456439000
H	3.216754000	3.902794000	6.698059000
C	3.306434000	0.828171000	8.973139000
H	3.679232000	-0.201244000	8.985982000
H	3.642057000	1.319312000	9.894314000
C	1.089801000	2.245534000	6.534652000
H	1.341364000	2.794770000	5.620333000
H	-0.001729000	2.180743000	6.615531000
C	1.325960000	0.148325000	7.700579000
H	0.236745000	0.061129000	7.790124000
H	1.757874000	-0.856774000	7.653969000
N	1.623408000	0.864527000	6.433915000
C	6.454094000	8.168309000	7.300389000
F	5.753253000	8.717396000	6.256016000
F	5.945082000	8.713039000	8.452563000